

1 **Bacterial Swarms exhibit a Protective Response to Intestinal Stress**

2 Weijie Chen^{1, 2, *}, Arpan De^{1, *}, Hao Li^{1, *}, Dana J. Lukin³, Wendy Szymczak⁴, Katherine Sun⁵,
3 Libusha Kelly⁶, Justin R. Wright⁷, Regina Lamendella⁸, Subho Ghosh¹, Daniel B. Kearns⁹, Zhen
4 He^{10, †}, Christian Jobin¹⁰, Xiaoping Luo^{1, ‡}, Arjun Byju¹, Shirshendu Chatterjee¹¹, Beng San
5 Yeoh^{12, §}, Matam Vijay-Kumar^{12, §}, Jay X. Tang², Sridhar Mani^{1, **}

6 ¹Department of Medicine, Genetics and Molecular Pharmacology, Albert Einstein College of Medicine,
7 1300 Morris Park Avenue, Bronx, NY 10461, USA;

8 ²Department of Physics, Brown University, 182 Hope Street, Providence, RI 02912, USA;

9 ³Jill Roberts Center for Inflammatory Bowel Disease, 1283 York Avenue, New York, NY 10065, USA;

10 ⁴Clinical Microbiology Laboratory, Montefiore Medical Center, 111 E 210th Street, Bronx, NY 10467,
11 USA;

12 ⁵Department of Pathology, NYU Langone Health, 560 First Avenue, New York, NY 10016, USA;

13 ⁶Department of Systems & Computational Biology, and Department of Microbiology & Immunology,
14 Albert Einstein College of Medicine, 1300 Morris Park Avenue, Bronx, NY 10461, USA;

15 ⁷Wright Labs, LLC, 419 14th Street, Huntington, PA 16652, USA;

16 ⁸Juniata College, 1700 Moore Street, Huntingdon, PA 16652, USA;

17 ⁹Department of Biology, Indiana University Bloomington, 107 S. Indiana Avenue, Bloomington, IN
18 47405, USA;

19 ¹⁰Department of Medicine, University of Florida, Gainesville, FL 32611, USA;

20 ¹¹Department of Mathematics, The City College of New York, 160 Convent Avenue, New York, NY
21 10031, USA;

22 ¹²UT-Microbiome Consortium, Department of Physiology & Pharmacology, University of Toledo, College
23 of Medicine & Life Sciences, 3000 Transverse Dr, Mail Stop 1008, Toledo, OH 43614, USA

24 * Equal contribution ** Corresponding author

25 † Present address: Department of Colorectal Surgery, The Sixth Affiliated Hospital of Sun Yat-Sen
26 University, 26 Yuancun Erheng Road, Tianhe district, Guangzhou, Guangdong, China

27 ‡ Present address: Institute of Chinese Materia Medica, Shanghai University of Traditional Chinese
28 Medicine, 1200 Cailun Road, Shanghai 201203, China

29 § Present address: Department of Physiology and Pharmacology, University of Toledo, College of Medicine
30 and Life Sciences, Toledo, OH 43614, USA

31

32 **Bacterial swarming is a conserved and distinct form of bacterial motility that is often**
33 **regulated differently than biofilm communities¹. While bacterial biofilms are associated with**
34 **pathogenesis and pathobiology of human diseases²⁻⁴, there are very few examples of**
35 **swarming behaviors that uniquely define or align with human pathophysiology⁵⁻⁷. Here we**
36 **report that bacterial swimmers are associated with protection against intestinal**
37 **inflammation in a murine model of acute colitis. Using feces in soft-agar plate assay, we**
38 **showed bacterial spreading harboring swimmers, is highly predictive of the presence of**
39 **intestinal stress in mice, pigs, and humans. From murine feces, we isolated a novel**
40 ***Enterobacter* swarming strain, SM3, which demonstrated significant protection from**
41 **intestinal inflammation when compared to its swarming deficient but swimming competent**
42 **transposon mutants in a DSS-induced intestinal inflammation model of mice. Known**
43 **commensal swimmers also protected against intestinal inflammation when compared to**
44 **swarming deficient isogenic mutants. When treated with SM3, its anti-inflammatory**
45 **properties paralleled a significant reduction of luminal oxygen concentration in colitic mice**
46 **as observed in real time using a microsensor probe. This led to a favorable anaerobic**
47 **environment conducive to the growth of beneficial anaerobes as demonstrated by 16S**
48 **profiling of feces. This work identifies a new paradigm in which intestinal stress, specifically**
49 **inflammation, allows for the emergence of swarming bacteria, which in turn can protect and**
50 **heal from intestinal inflammation.**

51 Swarming, driven by flagella, is a fundamental process in certain groups of bacteria characterized
52 by collective and rapid movement across a surface^{8,9}. This process offers bacteria a competitive
53 advantage in occupying specific niches (e.g., seeding colonization)¹⁰; however, the cost-benefits
54 to bacteria^{11,12} and consequences to its host or the environment remain primarily unknown⁷. Here
55 we show that bacterial swarming is a hallmark of a stressed intestine in mammals. In a mouse
56 model of intestinal stress, bacterial swimmers, when dosed in sufficient abundance, suppressed
57 intestinal inflammation. In the model of SM3 supplementation in mice with acute intestinal
58 inflammation, we observed reduced intestinal oxygen concentration and enrichment of beneficial
59 anaerobes in the feces. We posit that it is likely due to the act of swarming *in vivo* an anaerobic
60 environment is created, which is conducive to the growth of beneficial anaerobes associated with
61 mucosal healing.

62 To test whether bacterial swarming is associated with human and rodent gut health, we developed
63 a modified swarming assay using feces based on an established soft-agar plate assay utilized for
64 single species¹³. Since prototypical swarming bacteria (e.g., *Proteus mirabilis*, *Pseudomonas*
65 *aeruginosa*) are associated with virulence^{7,14}, we surmised that bacterial swarming might be well
66 represented in colonoscopy samples and feces from humans with bacterial virulence-associated
67 pathologies (e.g., intestinal inflammation)¹⁵. We obtained colonoscopy aspirates from individuals
68 with a progressive illness (inflammatory bowel disease - Crohn's and ulcerative colitis and other
69 common forms of intestinal stress like intestinal polyps^{16,17} as well as age and gender-matched
70 controls (those without a clinically active illness). Within our sampling pool, bacterial collective
71 spreading on soft agar was over-represented in cases with overt or clinically active intestinal stress
72 (Extended Data Fig. 1a-b). As a preliminary assessment, we judged the presence of bacterial

73 swarmer in feces by the bacterial spread with a surfactant layer on soft-agar followed by isolation,
74 identification by MALDI-TOF, and validation of its swarming motility (Extended Data Table 1).
75 Nevertheless, this approach might have precluded the selection of swarmer that do not produce
76 surfactant⁸. In this pilot evaluation, the specificity and positive predictive value of the test for
77 disease as defined was approximate, 88, and 89%, respectively. In comparison, the sensitivity and
78 negative predictive value of the test was only approximately 56 and 52%, respectively (Extended
79 Data Fig. 1c). Similarly, feces collected from pigs with active inflammatory bowel disease also
80 showed an increased prevalence of collective spreading and swarming as compared to control pigs
81 (Extended Data Fig. 1d). Together, these pilot data indicate that collective spreading and swarming
82 is a specific feature, and potentially a biomarker of an intestinal pathology as defined by harboring
83 active intestinal inflammation or polyps.

84 To identify the relevance of swarmer on host health, we focused on isolating endogenous
85 swarming bacteria residing in rodents and humans. An initial approach was to determine if a single
86 dominant swarming species could always be isolated from a polymicrobial culture (such as
87 mammalian feces). In a competitive swarming assay, a mix of different pure bacterial cultures
88 gave rise to a single bacterial species populating the leading edge of the swarm colony on agar
89 (Extended Data Fig. 2a-b). In congruence with our observation, a recent study has shown species
90 dependence on motility in niche dominance and stable coexistence when present in low abundance
91 in a mixed population¹⁸. Similarly, swarming assays using the pooled mouse or individual human
92 feces yielded single species of a dominant swarmer as identified by MALDI-TOF (Extended Data
93 Table 1; Extended Data Fig. 1e). To test whether swarming bacteria are also present in preclinical
94 models, we screened feces of mice exposed to DSS, a chemical colitogen causing acute colonic
95 inflammation^{19,20}. In a single experiment, we found three identical isolates from two different

96 mouse fecal specimens- Strain 1 from mice exposed to water and Strain 2 and 3 from mice exposed
97 to dextran sulfate sodium (DSS), respectively (Fig. 1a). Swarming (in feces) was uniformly absent
98 in vehicle exposed mice (Extended Data Fig. 1e). We picked the edge of the swarm colonies (as
99 marked on Fig. 1a), then serially passaged twice on 1% agar from a single colony, and
100 subsequently re-tested for swarm behavior on 0.5% agar plates (Fig. 1b). Strain 3 swarmed
101 significantly faster compared to Strain 1 and 2. Interestingly, 16S rRNA gene analysis and Multi
102 Locus Sequence Typing (Fig. 1c) identified the isolated strains to be closest to *Enterobacter*
103 *asburiae*. Whole-genome sequence comparison of these *Enterobacter* strains (Fig. 1d) with related
104 taxa *Enterobacter asburiae* and *Enterobacter cloacae*, revealed that all the three strains isolated
105 here were “nearly identical” (>99% identical, Supplementary Discussion) and phylogenetically
106 distinct from the reference strains. Taken together, using an agar-based assay to isolate dominant
107 swarmers from a heterogenous culture, we were able to isolate nearly identical strains with striking
108 differences in their swarming potential. Strain 1 (*Enterobacter* sp. SM1) originated from feces of
109 the vehicle (water) treated mice, while strain 2 (*Enterobacter* sp. SM2) and strain 3 (*Enterobacter*
110 sp. SM3) originated from feces of DSS-induced colitis mice. Interestingly, a quantitative PCR
111 sequencing-based approach to accurately identify SM1 or SM3 like bacteria in feces showed an
112 increase in its abundance during the evolution of DSS-induced colitis. The proportion of mice with
113 high copy number values (>10,000 DNA copy number / μ L) was significantly higher in the DSS
114 group than water only group (Extended Data Fig. 1f).

115 To determine the functional consequence of bacterial swarming in the host, we administered the
116 “near-identical” swarming competent SM1 or SM3 strains to mice with DSS-induced colitis. Both
117 strains possess the same growth rate and swim speed; however, in comparison with SM1, SM3 is
118 a hyperswarmer (Extended Data Fig. 3a-e; Supplementary Video 1). In contrast to that observed

119 with SM1, SM3 significantly protected mice from intestinal inflammation (Fig. 2a-f). Specifically,
120 SM3 significantly protected from body weight loss (Fig. 2a), increased colon length (Fig. 2b),
121 reduced the colonic inflammation score (Fig. 2d), and had reduced expression of pro-inflammatory
122 mediators compared to vehicle-treated colitic mice (Fig. 2e-f). To test the mucosal healing capacity
123 of swarming bacteria, we administered strains SM1 and SM3 to mice during the recovery phase
124 of DSS exposure²¹. When compared to the vehicle, SM3 significantly improved weight gain and
125 colon length with reduced total inflammation and fibrosis at the microscopic level (Extended Data
126 Fig. 4). We did not find differential regulation of any virulence associated genes between SM1 and
127 SM3 strains when collected from swarming plates (Extended Data Fig. 3k-l). SM3 and its isogenic
128 transposon mutants (SM3_18 and SM3_24) that only differed in swarming potential but not growth
129 rate, surfactant production, or swimming speed (Extended Data Fig. 3f-j), were administered to
130 mice exposed to DSS. SM3, but not the swarming deficient mutants (SM3_18 and SM3_24),
131 showed significant protection against weight loss, colon length, and inflammation (Fig. 2g-i).
132 During the course of experiment, on day 4, the levels of SM3 and its mutants present in feces were
133 not significantly different (Extended Data Fig. 5a-b). We chose to enumerate bacterial levels in
134 feces on day 4 due to the equivalent pathological conditions of mice, as defined by weight change,
135 when treated with different strains. To identify, if the loss of protection by SM3_18 could be
136 related to slightly higher levels of its presence compared to SM3, although not significant, we
137 performed a dose attenuation study. Even at low dose, the levels of inflammation as represented
138 by lipocalin concentration and the weight loss was not significantly different from the vehicle
139 group, negating the possibility of any associated virulence that may attribute to loss of protection
140 by SM3_18 (Extended Data Fig. 5e-f). Furthermore, we did not find significant difference of any
141 virulence associated gene between SM3, and SM3_18, and SM3_24 strains when collected from

142 swarming plates. Thus, in our mutants, pleiotropic effects of gene mutations on virulence is not a
143 cause for lack of protection from inflammation. Together, however, these data indicated that SM3
144 with swarming properties, as opposed to swarming-deficient strains, is associated with anti-
145 inflammatory activity.

146 To determine if the anti-inflammatory role of SM3 is dependent on the conventional intestinal
147 microbiome composition, germ-free mice transferred to specific pathogen-free conditions
148 (GF/SPF) and exposed to DSS-induced colitis, were treated with SM3. This strain was unable to
149 protect against intestinal inflammation in GF/SPF mice (Fig. 3a). We analyzed fecal samples of
150 colitic mice (conventional and GF/SPF) with SM3 administered using 16S rRNA gene profiling.
151 In contrast to GF/SPF mice, conventional mice feces showed specific enrichment of anaerobes
152 belonging to the family S24-7 and Lactobacillaceae within SM3 treated mice when compared to
153 vehicle mice (Fig. 3b). Specifically, in conventional mice, we found a significant increase in the
154 abundance of S24-7 with SM3 gavage compared to vehicle in DSS exposed mice (Fig. 3c). In mice
155 not exposed to DSS, the levels of S24-7 bacteria remain stable in SM3 treated group when
156 compared with the untreated group (Fig. 3c). Within DSS exposed conventional mice, we observed
157 that enriched S24-7 negatively co-occurred with pathogenic taxa such as the
158 Peptostreptococcaceae and Enterobacteriaceae (Fig. 3d). Of importance, feces from GF/SPF mice
159 exposed to DSS and treated with SM3 also showed enrichment of anaerobic and microaerophilic
160 taxa compared to the vehicle group (Extended Data Fig. 6). By contrast, the fecal microbiota of
161 vehicle group was enriched in taxa that are aerobic and/or facultative anaerobic.

162

163 The enrichment of certain specific anaerobes when treated with SM3 suggests a reduction in
164 oxygen content in the intestine; however, during inflammation, the median oxygen concentration

165 in the lumen increases (Extended Data Fig. 7a). We determined the oxygen concentrations within
166 the intestinal lumen of mice at various lengths along the colon. In control conventional C57BL/6
167 mice, the colonic lumen is uniformly “hypoxic or anoxic”. In colitic mice, however, we found a
168 significant increase in the oxygen levels (ppm) in the colonic lumen (measured at different lengths
169 from 0.5 to 2 cm proximal to the anal verge) (Extended Data Fig. 7a). In DSS exposed mice treated
170 with SM3, we observed a significant reduction in the luminal oxygen concentrations when
171 compared to the mice that were treated with SM1 and the swarming deficient mutant strains
172 (Extended Data Fig. 7b-c). SM3_18 and SM3_24 did not significantly affect oxygen
173 concentrations compared with vehicle control (Extended Data Fig. 7c).

174 Additionally, we found that the swarming behavior of SM3 is dependent on oxygen concentration
175 (Extended Data Fig. 7d), which in turn reduces the oxygen levels at a significantly higher rate than
176 the slow swarming variants (Extended Data Fig. 7e). Hence, we hypothesize that the swarming
177 activity of SM3 *per se* is likely to occur *in vivo*, which might contribute to reducing the median
178 oxygen concentrations in the intestinal lumen. These results show that SM3, a hyperswarmer
179 relative to SM1, but not swarming deficient strains or less dominant swarmers (i.e., SM1),
180 consume oxygen rapidly. Collectively, our data suggest that SM3 and healing induced oxygen
181 depletion in mice with colitis probably contributes towards establishing an anaerobic
182 microenvironment.

183 To generalize this concept across multiple strains, mice with DSS induced colitis were
184 administered *B. subtilis* 3610 (wildtype)²² or its swarming deficient *swrA* isogenic mutant DS215²³
185 using the identical protocol as that used for SM3. In comparison with strain DS215, the wildtype
186 significantly protected mice from intestinal inflammation (Fig. 4a-e). Similarly, swarming *Serratia*
187 *marcescens* Db10, in contrast to the swarming deficient JESM267 isogenic mutant²⁴, protected

188 against inflammation in the identical mouse model (Fig. 4f-h). The bacterial levels in feces,
189 collected on day 4 were not different compared to its respective mutant (Extended Data Fig. 5c-
190 d). Incidentally, a clinical strain of *S. marcescens* (isolated from the surface washing of a human
191 dysplastic polyp) also protected against DSS induced inflammation in mice (Supplementary
192 Discussion). Together, our results confirm that from a diverse set of genes and pathways altered
193 in different bacterial strains, the swarming phenotype of bacteria correlates with protection against
194 inflammation. Similar to SM3, the swarming strains of *Bacillus* and *Serratia* deplete oxygen
195 significantly faster than the isogenic non-swarming strains *in vitro* (Extended Data Fig. 7f-g).
196 These data suggest that a possible common mechanism might exist among swimmers, in that, via
197 depletion of local oxygen concentrations, they all induce a favorable anaerobic environment. Also,
198 the intestinal mucosa is relatively uneven during inflammation due to loss of mucin²⁵. We
199 conjectured, therefore, that swimmers might have an added advantage in niche dominance on
200 inflamed tissue. Indeed, a mucosal race assay (Supplementary Discussion) showed that swarming
201 bacteria finds an advantage in motility on a colitic mucosa compared to normal mucosa
202 (Supplementary Video 2-4).

203 Together these studies demonstrate that intestinal inflammation promotes a protective niche for
204 swarming bacteria, as demonstrated by *in vitro* assays. The inflammatory milieu provides a
205 permissive environment for stress adaptation and swarming behavior. Swarming bacteria, when
206 present in sufficient abundance, deplete luminal oxygen content and allow for the intestine to re-
207 establish conditions conducive to the growth of beneficial anaerobes. We cannot exclude other
208 direct or indirect effects of the swarming strain on mucosal inflammation and healing. However,
209 if present, it would assist in suppressing host inflammation in conjunction with re-establishing
210 homeostatic anaerobiosis in the gut (Extended Data Fig. 8).

211 Furthermore, our studies demonstrate the potential for a new personalized “probiotic” approach
212 stemming from the ability to isolate and bank swarming microbes during colitis flares. These could
213 be stored and provided back to the same individuals to prevent colitic episodes or as a therapeutic
214 during acute colitis. In summary, our work demonstrates the unique and unprecedented role that
215 bacterial swarming plays in intestinal homeostasis and the potential clinical treatment of
216 inflammatory bowel diseases.

217

Figure 1

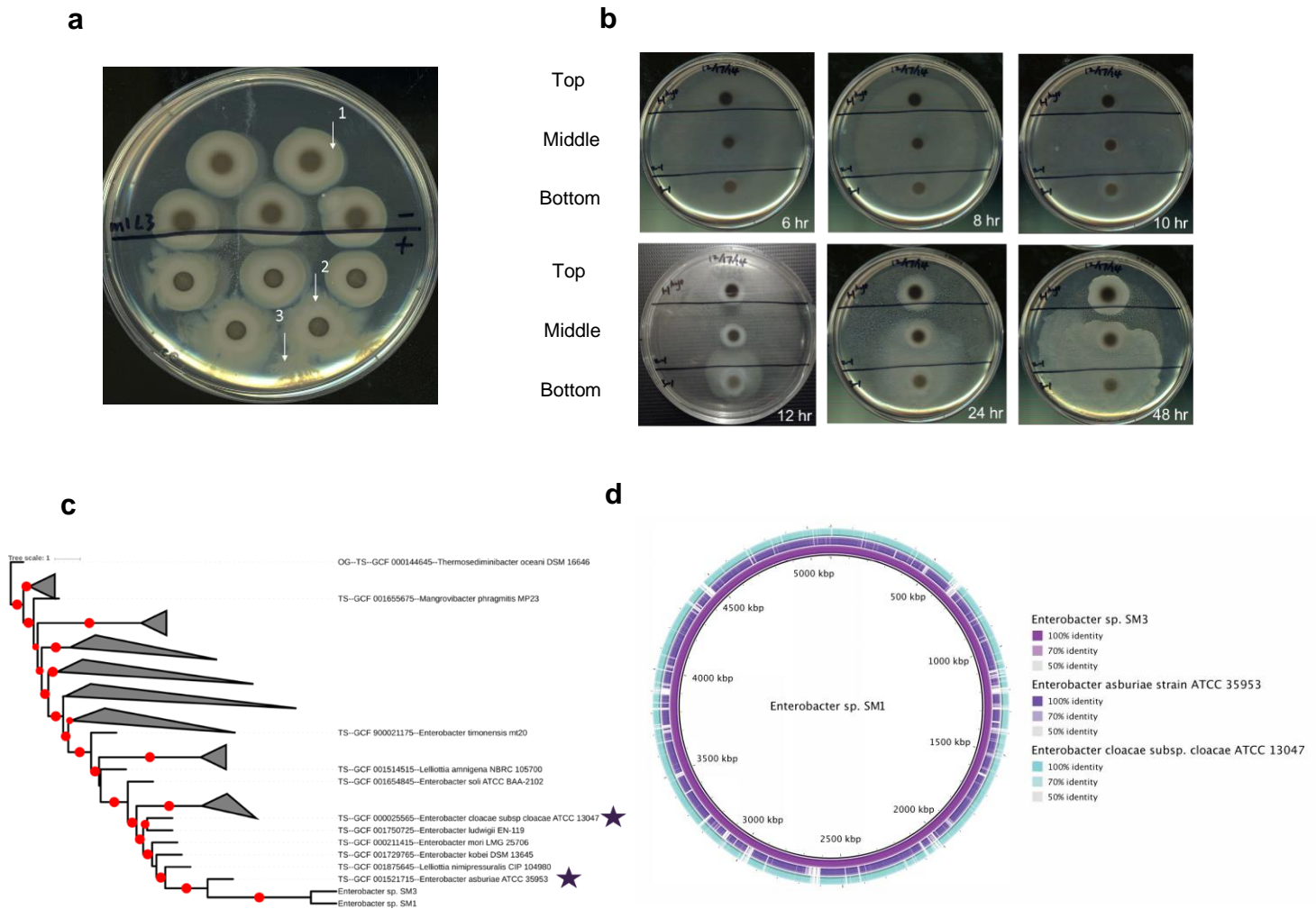


Figure 1 | Isolation and characterization of *Enterobacter* sp. a, Five replicate fecal spots from pooled fecal pellets of mice administered water (above black line) or 3% DSS water (below black line) ($n = 3$, day 7). The white arrows indicate 1, swarm edge isolation from control feces (SM1); 2, swarm edge isolation from feces of mice exposed to DSS (SM2); 3, swarm colony isolation from spontaneous “burst” activity from feces at 24h from plating (SM3). The mouse experiments were repeated at least twice. **b**, The bacterial clones isolated from **a** were replated as pure strains on 0.5% LB agar and the swarming assay performed over time. Two solid black marker lines divide each plate into 3 regions, holding spots of the 3 strains – Top: Strain 1 (SM1), Middle: Strain 2 (SM2), Bottom: Strain 3 (SM3). These strains have been repeatedly (≥ 25 times) plated in swarming assays from all aliquots stored from the original isolation (August 2014) and the results confirm that SM3 is a stable hyperswarmer. **c**, Phylogenetic tree showing multi-locus sequencing typing-based genetic relatedness between *Enterobacter* sp. SM1, SM3 and reference genomes. Tree was generated with autoMLST (CITE) and drawn using iTOL (CITE). Red dots indicate bootstrap support > 0.8 . Stars represent related strains used for comparison with the genome sequences of SM1 and SM3 in panel **d**. **d**, Genome comparison of related *Enterobacter* strains. *Enterobacter* sp. SM1 was compared to *Enterobacter* sp. SM3 (purple) and the related strains *Enterobacter asburiae* ATCC 35953 (violet) and *Enterobacter cloacae* ATCC 13047 (cyan), and plotted in BLAST Ring Generator (BRIG) <http://brig.sourceforge.net/>; PMID: 21824423. DSS, Dextran Sulfate Sodium; LB, Luria-Bertani broth.

Figure 2

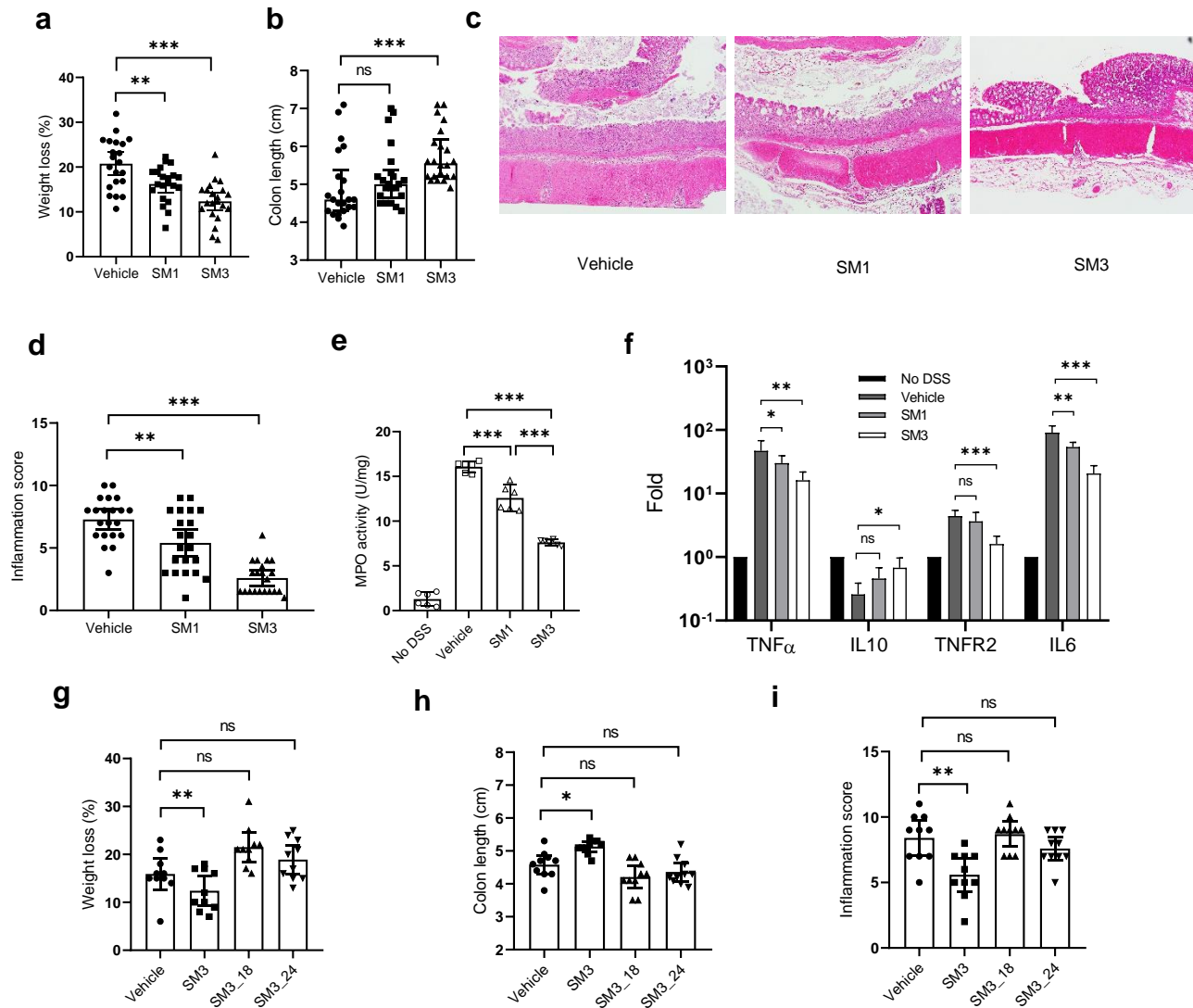


Figure 2 | Effects of *Enterobacter* sp. SM strains on DSS induced colitis in C57BL/6 mice. **a-f**, 8-week-old mice were exposed to DSS water and treated with vehicle (LB), SM1 or SM3 by oral gavage for 10 days. **a-b** indicates weight loss (**a**) and colon length (**b**) ($n = 21$ per treatment group). **c**, Representative images (100x magnification) of H&E stained colonic section treated with vehicle (left), SM1 (middle) and SM3 (right). **d**, Inflammation score ($n = 21$ per treatment group). **e-f**, In a separate experiment, myeloperoxidase (MPO) enzyme activity was determined ($n = 3$, each in duplicate) (**e**). Colon total RNA ($n = 4$) was isolated and reverse transcribed to cDNA. RT-qPCR data show fold induction of mRNA (TNF α , IL10, TNFR2, IL6). PCR was repeated in quadruplicate. The expression was normalized to internal control, TBP. The entire experiment was repeated $n = 2$ for reproducibility (**f**). **g-i**, In a separate experiment, C57BL/6 mice (8-week old) were exposed to DSS water and administered vehicle (LB), SM3, or its mutants (SM3_18 or SM3_24) for 10 days. **g-i** indicates weight loss (**g**), colon length (**h**) and inflammation score (**i**) ($n = 10$ per treatment group). Unless otherwise noted, data are represented as mean and 95% CI, and significance tested using one-way ANOVA followed by Tukey's post hoc test. **c**, data represented as median and interquartile range, and significance tested using Kruskal-Wallis followed by Dunn's multiple comparisons test. * $P < 0.05$; ** $P < 0.01$; *** $P < 0.001$; ns, not significant. H&E, Hematoxylin and Eosin; TBP, TATA-Box Binding Protein; CI, Confidence Interval.

Figure 3

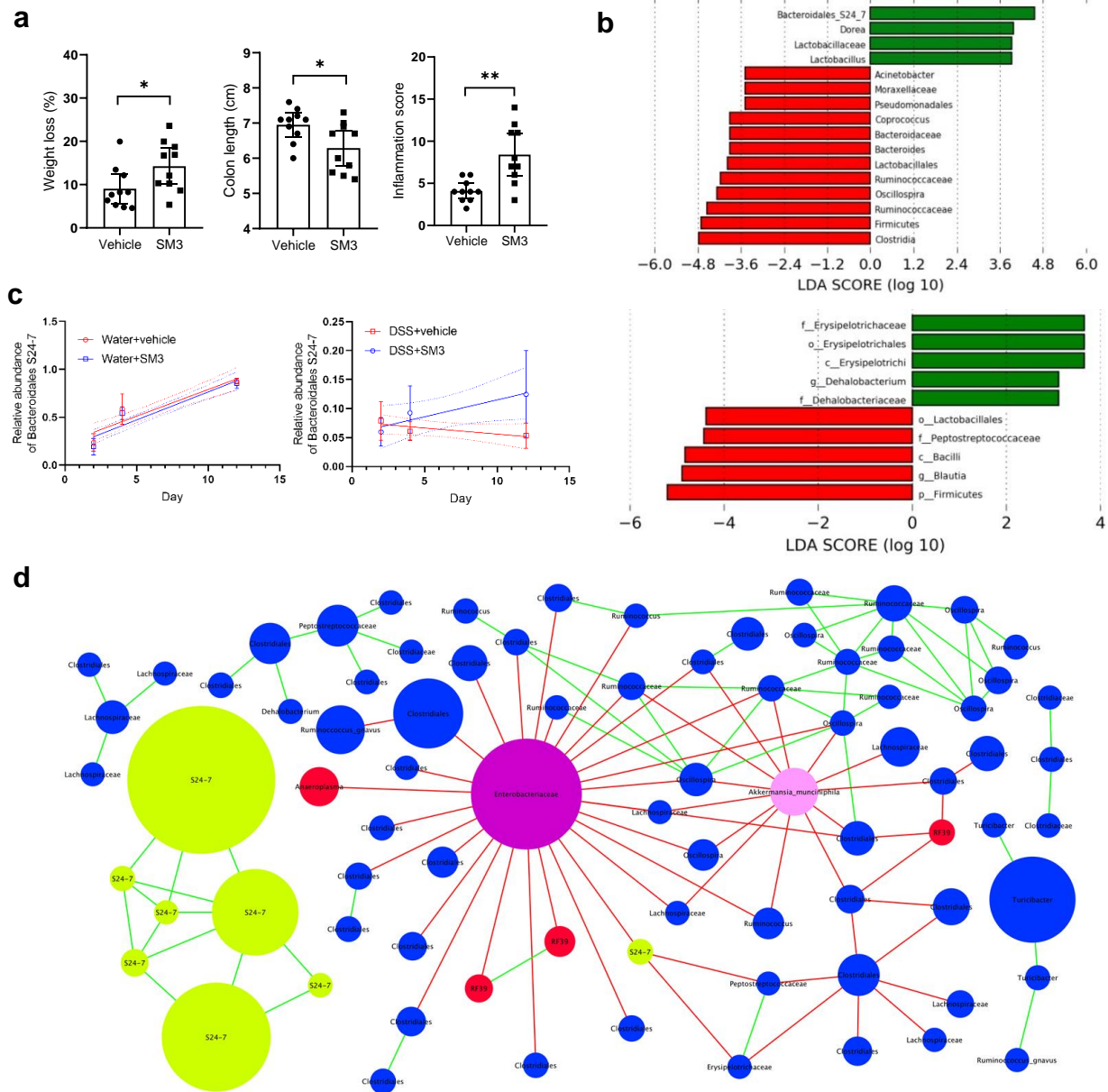


Figure 3 | Effects of SM3 on the intestinal microbiota of GF/SPF and conventional mice. **a**, C57BL/6 GF/SPF mice (5-week old) were exposed to DSS water and treated with vehicle (LB) or SM3 for 6 days. **a** indicates weight loss (left), colon length (middle), and inflammation score (right) ($n = 10$ per treatment group). **b**, Linear discriminant analysis (LDA) Effect Size (LEfSe) plot of taxonomic biomarkers identified using feces of SM3 treated conventional ($n = 10$) (upper) and GF/SPF ($n = 10$) (lower) colitic mice on day 12 and day 6, respectively, as compared to vehicle ($n = 10$). Green and red bars indicate bacterial enrichment within SM3 treated and vehicle group respectively. All taxa that yielded an LDA score >3.0 are presented. **c**, Relative abundance of S24-7 in the feces from DSS (right) and control (left) mice treated with SM3 or vehicle ($n = 8$ per treatment group). Linear regression line was fit to show the trend of the change (dotted lines show the 95% confidence bands). The slope of the SM3 treated group is similar to vehicle in water control group ($P = 0.7827$), but significantly different in DSS group ($P = 0.0182$). **d**, Co-occurrence network plot showing strong positive and negative correlations (Spearman's $\rho > 0.7$) between OTU abundances. Each node represents a single OTU and the size of each node is proportional to the relative abundance of each OTU. Green lines connecting two nodes indicate a strong positive correlation (spearman's $\rho > 0.7$) between the taxa, whereas red lines indicate a strong negative correlation (spearman's $\rho < -0.7$) between the taxa. Unless otherwise noted, data are represented as mean and 95% CI, and significance tested using a two-tailed Student's t-test. OTU, Operational Taxonomic Unit; GF/SPF, Germ-Free mice transferred to specific pathogen free conditions.

Figure 4

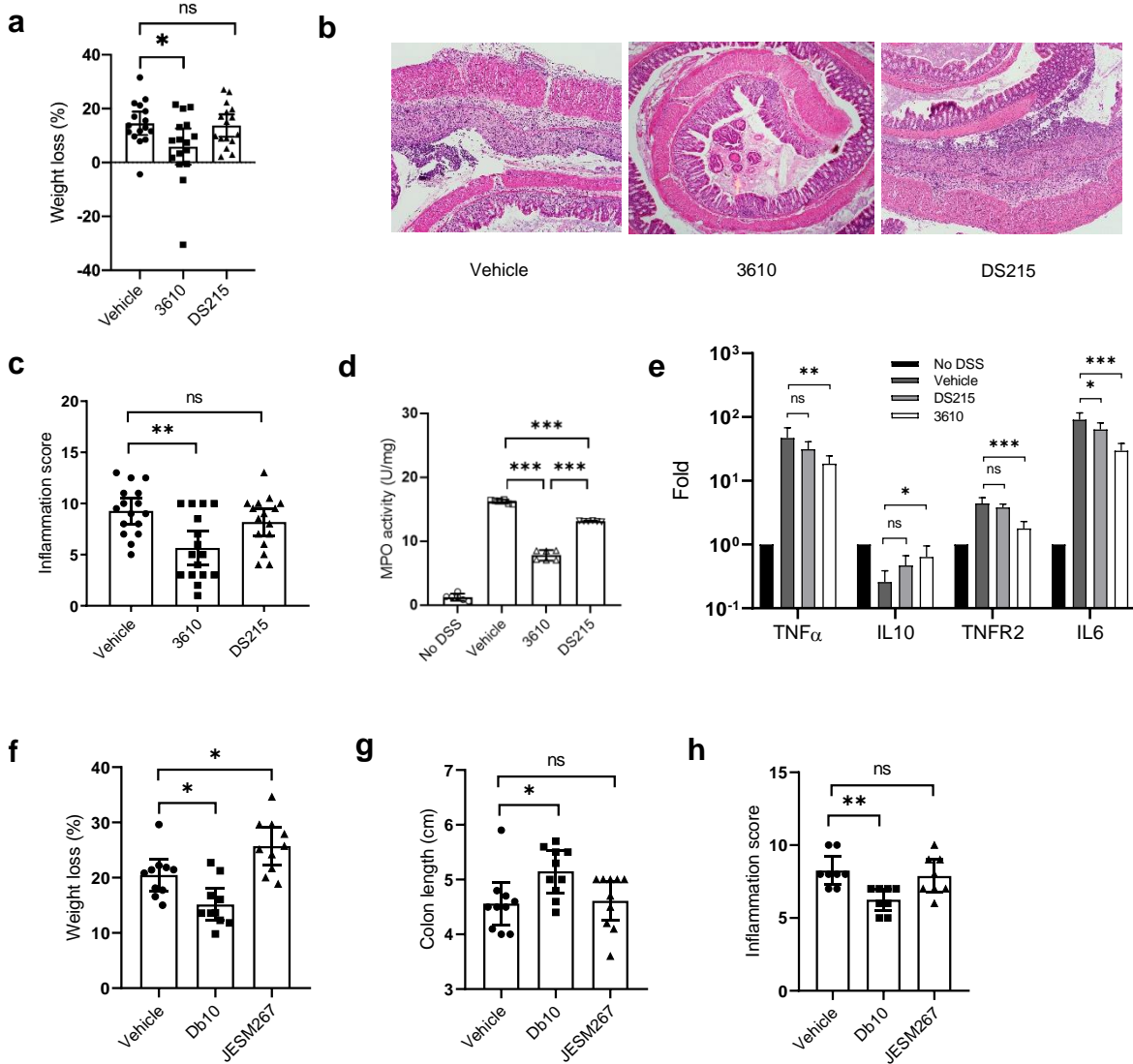


Figure 4 | Effects of *B. subtilis* and *S. marcescens* on DSS induced colitis in C57BL/6 mice. a-e, 8-week old mice were exposed to DSS water and treated with vehicle (LB), *B. subtilis* 3610 or *B. subtilis* DS215 by oral gavage for 10 days. **a**, Weight loss (n = 16 per treatment group). **b**, Representative images (100x magnification) of H&E stained colonic section treated with vehicle (left), 3610 (middle) and DS215 (right). **c**, Inflammation score (n = 16 per treatment group). **d-e**, In a separate experiment, myeloperoxidase (MPO) enzyme activity was determined (n = 3, each in duplicate) (**d**). Colon total RNA (n = 4) were isolated and reverse transcribed to cDNA. RT-qPCR data show fold induction of mRNA (TNF α , IL10, TNFR2, IL6). PCR was repeated in quadruplicate. The expression was normalized to internal control, TBP. The entire experiment was repeated n = 2 for reproducibility (**e**). **f-h**, In a separate experiment, C57BL/6 mice (8-week old) were exposed to DSS water and administered vehicle (LB), *S. marcescens* Db10 or *S. marcescens* JESM267 for 10 days. **f-h** indicates weight loss (**f**), colon length (**g**) and inflammation score (**h**) (n = 10 per treatment group except for **h**, for which n = 8; two colon specimens per group were used for other experiments). Unless otherwise noted, data represented as mean and 95% CI, and significance tested using one-way ANOVA followed by Tukey's post hoc test. **g**, data represented as median and interquartile range, and significance tested using Kruskal-Wallis followed by Dunn's multiple comparisons test.

218 **References**

- 219 1 Verstraeten, N. *et al.* Living on a surface: swarming and biofilm formation. *Trends*
220 *Microbiol* **16**, 496-506, doi:10.1016/j.tim.2008.07.004 (2008).
- 221 2 Dejea, C. M. *et al.* Microbiota organization is a distinct feature of proximal colorectal
222 cancers. *Proc Natl Acad Sci U S A* **111**, 18321-18326, doi:10.1073/pnas.1406199111
223 (2014).
- 224 3 Villanueva, M. T. Metabolism: Bacterial biofilms may feed colon cancer. *Nat Rev Cancer*
225 **15**, 320, doi:10.1038/nrc3970 (2015).
- 226 4 Johnson, C. H. *et al.* Metabolism links bacterial biofilms and colon carcinogenesis. *Cell*
227 *Metab* **21**, 891-897, doi:10.1016/j.cmet.2015.04.011 (2015).
- 228 5 Breidenstein, E. B., de la Fuente-Nunez, C. & Hancock, R. E. *Pseudomonas aeruginosa*: all
229 roads lead to resistance. *Trends Microbiol* **19**, 419-426, doi:10.1016/j.tim.2011.04.005
230 (2011).
- 231 6 Butler, M. T., Wang, Q. & Harshey, R. M. Cell density and mobility protect swarming
232 bacteria against antibiotics. *Proc Natl Acad Sci U S A* **107**, 3776-3781,
233 doi:10.1073/pnas.0910934107 (2010).
- 234 7 Allison, C., Emody, L., Coleman, N. & Hughes, C. The role of swarm cell differentiation and
235 multicellular migration in the uropathogenicity of *Proteus mirabilis*. *J Infect Dis* **169**, 1155-
236 1158, doi:10.1093/infdis/169.5.1155 (1994).
- 237 8 Kearns, D. B. A field guide to bacterial swarming motility. *Nat Rev Microbiol* **8**, 634-644,
238 doi:10.1038/nrmicro2405 (2010).
- 239 9 Be'er, A. & Ariel, G. A statistical physics view of swarming bacteria. *Mov Ecol* **7**, 9,
240 doi:10.1186/s40462-019-0153-9 (2019).
- 241 10 Barak, J. D., Gorski, L., Liang, A. S. & Narm, K. E. Previously uncharacterized *Salmonella*
242 *enterica* genes required for swarming play a role in seedling colonization. *Microbiology*
243 **155**, 3701-3709, doi:10.1099/mic.0.032029-0 (2009).
- 244 11 Butler, M. T., Wang, Q. & Harshey, R. M. Cell density and mobility protect swarming
245 bacteria against antibiotics. *Proceedings of the National Academy of Sciences of the*
246 *United States of America* **107**, 3776-3781, doi:10.1073/pnas.0910934107 (2010).
- 247 12 Finkelshtein, A., Roth, D., Ben Jacob, E. & Ingham, C. J. Bacterial Swarms Recruit Cargo
248 Bacteria To Pave the Way in Toxic Environments. *mBio* **6**, doi:10.1128/mBio.00074-15
249 (2015).
- 250 13 Morales-Soto, N. *et al.* Preparation, imaging, and quantification of bacterial surface
251 motility assays. *J Vis Exp*, doi:10.3791/52338 (2015).
- 252 14 Overhage, J., Bains, M., Brazas, M. D. & Hancock, R. E. Swarming of *Pseudomonas*
253 *aeruginosa* is a complex adaptation leading to increased production of virulence factors
254 and antibiotic resistance. *J Bacteriol* **190**, 2671-2679, doi:10.1128/jb.01659-07 (2008).
- 255 15 Yang, Y. & Jobin, C. Microbial imbalance and intestinal pathologies: connections and
256 contributions. *Dis Model Mech* **7**, 1131-1142, doi:10.1242/dmm.016428 (2014).
- 257 16 Jass, J. R. Hyperplastic-like polyps as precursors of microsatellite-unstable colorectal
258 cancer. *Am J Clin Pathol.* **119**, 773-775 (2003).
- 259 17 Crespo-Sanjuán, J. *et al.* Early detection of high oxidative activity in patients with
260 adenomatous intestinal polyps and colorectal adenocarcinoma: myeloperoxidase and

- 261 oxidized low-density lipoprotein in serum as new markers of oxidative stress in colorectal
262 cancer. *Lab Med.* **46**, 123-135 (2015).
- 263 18 Gude, S. *et al.* Bacterial coexistence driven by motility and spatial competition. *Nature*
264 **578**, 588-592, doi:10.1038/s41586-020-2033-2 (2020).
- 265 19 Perse, M. & Cerar, A. Dextran sodium sulphate colitis mouse model: traps and tricks. *J*
266 *Biomed Biotechnol* **2012**, 718617, doi:10.1155/2012/718617 (2012).
- 267 20 Chassaing, B., Aitken, J. D., Malleshappa, M. & Vijay-Kumar, M. Dextran sulfate sodium
268 (DSS)-induced colitis in mice. *Curr Protoc Immunol* **104**, Unit 15 25,
269 doi:10.1002/0471142735.im1525s104 (2014).
- 270 21 Suzuki, K. *et al.* Pivotal Role of Carbohydrate Sulfotransferase 15 in Fibrosis and Mucosal
271 Healing in Mouse Colitis. *PLoS One* **11**, e0158967, doi:10.1371/journal.pone.0158967
272 (2016).
- 273 22 Kearns, D. B. & Losick, R. Swarming motility in undomesticated *Bacillus subtilis*. *Mol*
274 *Microbiol* **49**, 581-590 (2003).
- 275 23 Kearns, D. B., Chu, F., Rudner, R. & Losick, R. Genes governing swarming in *Bacillus subtilis*
276 and evidence for a phase variation mechanism controlling surface motility. *Mol Microbiol*
277 **52**, 357-369, doi:10.1111/j.1365-2958.2004.03996.x (2004).
- 278 24 Pradel, E. *et al.* Detection and avoidance of a natural product from the pathogenic
279 bacterium *Serratia marcescens* by *Caenorhabditis elegans*. *Proc Natl Acad Sci U S A* **104**,
280 2295-2300, doi:10.1073/pnas.0610281104 (2007).
- 281 25 Sasaki, Y., Fukuda, S., Mikam, T. & Hada, R. Endoscopic quantification of mucosal surface
282 roughness for grading severity of ulcerative colitis. *Digestive Endoscopy* **20**, 67-72,
283 doi:10.1111/j.1443-1661.2008.00778.x (2008).
- 284

285 **Acknowledgements**

286 We thank Steve Almo, Cait Costello, Jeffrey Pessin, Matthew R. Redinbo and John March for
287 valuable discussions. We also thank Brad Tricomi for developing the assay “Cytotoxicity of DSS
288 on Caco-2 cell lines in the presence or absence of viable SM3 cells”, Ehsan Khafipour for
289 providing pig specimens (feces) and performing clinical scoring of histopathology, Edward Nieves
290 for performing LC-MS/MS identification of SM3 flagella, Cori Bargmann at Rockefeller University
291 for gifting us the bacterial strains *Serratia marcescens* Db10 and *Serratia marcescens* JESM267,
292 and Barry Bochner at Biolog Inc., California for Biochemical characterization and antimicrobial
293 resistance profile of *Enterobacter* sp. SM1, SM2 and SM3. Additional invaluable assistance was
294 obtained from Amanda Beck DVM (Histology and Comparative Pathology Core, Albert Einstein
295 College of Medicine, Bronx, NY), Olga C. Arionadis, Thomas Ullmann and Azal Al Ani
296 (Department of Medicine, Albert Einstein College of Medicine, Bronx, NY), Winfred Edelmann
297 and Eleni Tosti (Department of Cell Biology, Albert Einstein College of Medicine, Bronx, NY).
298 The studies presented here were supported in part by the Broad Medical Research Program at
299 CCFA (Crohn’s & Colitis Foundation of America; Grant# 362520) (to S.M.); NIH R01 CA127231;
300 CA 161879; 1R01ES030197-01 and Department of Defense Partnering PI (W81XWH-17-1-0479;
301 PR160167) (S.M.), Diabetes Research Center Grant (P30 DK020541); Cancer Center Grant
302 (P30CA013330 PI: David Goldman); 1S10OD019961-01 NIH Instrument Award (PI: John
303 Condeelis); LTQ Orbitrap Velos Mass Spectrometer System (1S10RR029398); and NIH CTSA (1
304 UL1 TR001073). Peer Reviewed Cancer Research Program Career Development Award from the
305 United States Department of Defense (CA171019, PI: Libusha Kelly).

306 **Author Contributions**

307 H.L., S.M. conceptualized the discovery. H.L., D.K., W.C., J.T., S.M. designed and executed the
308 swarming assays. D.L. was the Principal Investigator of the Clinical Study and provided
309 specimens. L.K. performed genome assembly and annotation. J.W., R.L., S.M. designed and
310 executed all the 16S, metagenomic and strain-specific PCR assays. A.D. designed; A.D., W.C.,
311 S.M., S.G. characterized bacterial mutants. B.S.Y. and M.V-K. performed several swarming repeat
312 assays and performed animal studies for reproducibility. A.D., H.L., W.C. and S.M. wrote and
313 edited the paper. S.C. and W.C. performed statistical analyses. X.L. assisted H.L. in mouse model
314 studies. S.G. has performed a single independent mice model study. A.B. analyzed the clinical data
315 and revised the paper. K.S. did the histological preparations and examination. C.J. and Z.H.
316 performed gnotobiotic mouse model studies. W.S. identified bacteria strains using MALDI-TOF.

317 **Competing Financial Interests**

318 Sridhar Mani, Libusha Kelly, and Hao Li filed a U.S. patent application (Application No.
319 62237657). Other authors declare no competing financial interests.

320 **Materials and Correspondence**

321 Sridhar Mani, MD **E-mail:** sridhar.mani@einstein.yu.edu

322

323 **Methods**

324 **Isolation and identification of bacterial swimmers from feces.** Swarming assay was performed
325 on Luria Bertani (LB) swarming agar medium (10 g/L tryptone (Sigma), 5 g/L yeast extract
326 (Acumedia) 10 g/L NaCl (Fisher), 5 g/L Agar (RPI)) with some modifications to an established
327 method¹³. To isolate a singular dominant swimmer from a polymicrobial mix of bacteria (such as
328 feces), we initially focused on developing an assay to isolate swimmers using known polymicrobial
329 mixed cultures of bacteria. Single bacterial species (up to seven strains belonging to different taxa)
330 grown in LB [OD₆₀₀ of 1.0-1.3] were mixed in a 1:1 ratio and, 5µL of this mix was spotted on
331 0.5% agar plates. Following air drying at room temperature, the plates were and incubated at 37°C,
332 40% RH (relative humidity) for 10 hours. Bacterial swimmer front was swabbed using a sterile tooth-
333 pick from the edge of swarming colony at different locations (see arrows, Extended Data Fig. 2)
334 and after re-streaking on separate agar plates and scaled by growth in LB, samples were identified
335 using Matrix Assisted Laser Desorption and Ionization-Time of Flight (MALDI-TOF). Swimmers
336 or hyperswimmers present in the fecal or colonoscopic samples were isolated and determined using
337 an identical approach. Fecal pellets and/or colonoscopy aspirates from the clinic and/or feces of
338 mice and pigs were collected in sterile tubes, and freshly prepared and used for swarming assays
339 before freezing in small aliquots at -80°C. Feces from stressed intestinal model of pigs²⁶ were
340 obtained on dry ice from Ehsan Khafipour at University of Manitoba Winnipeg, Canada. Five (5)
341 µL of homogenized feces in Phosphate buffered saline PBS, pH 7.2 (100 mg/mL) or colonoscopic
342 aspirates were spotted on swarming agar plates (optimized to 0.5% agar) and were incubated at
343 37°C and 40% RH, for 120 hours. Most bacterial swimmers, however, were detected within the
344 first 48-72h from incubation. Dominant swimmers from the edge of the colony were identified

345 using MALDI-TOF. Once identified, cells from the same aliquot were plated on to 1.5% LB agar
346 and serially passaged from a single colony to obtain a pure culture of the strain.

347 **Bacterial swarming and time-lapse imaging.** Swarming ability of a single bacterial species using
348 a pure culture of *Enterobacter* sp. SM1 and its isogenic mutant, *Enterobacter* sp. SM3 and its
349 transposon mutants, *Serratia marcescens* Db10 and JESM267, clinical isolate of *Serratia*
350 *marcescens*, *Bacillus subtilis* 3610 and its isogenic mutant DS215 was always determined on LB
351 swarming agar at 37°C and 40% RH prior to any experiments using these strains. *B. subtilis* 3610
352 and its isogenic mutant were compared on LB swarming agar containing 0.7% agar²⁷. Briefly, 2
353 µL of an overnight culture grown in LB medium from a glycerol stock was spotted on swarming
354 agar plate, followed by air drying at room temperature and incubating the plate overnight as stated
355 above. Freshly made swarming agar plates, no more than 12 hours old when stored at 4°C, were
356 used throughout the study. In order to capture real time swarming motility, a temperature and
357 humidity controlled incubator equipped with time lapse photography was built (see accompanying
358 publication on Nature Protocol Exchange for detailed protocol, doi:10.21203/rs.2.9946/v1). As
359 swarming is dependent upon RH⁸, we used an optimized RH of 40% that allowed image capturing
360 without condensation on the lid of the Petridish. Unless otherwise stated, swarming potential of
361 isogenic strains was always compared on the same swarming agar plate to nullify the difference
362 due to the condition of the medium, which may vary between plates. Swarming area was calculated
363 using a python based script (available online, via Nature Protocol Exchange) to identify the
364 swarming edge using the time-lapse images. Swarming under anerobic condition (0.1 ppm) and
365 10% oxygen (3.3 ppm) were performed at 37°C and 40% RH in an anaerobic chamber (Coy Labs
366 Inc.). In order to compare swarming motility between two strains, bacterial cultures were

367 inoculated on a single plate and the colony areas were measured when the faster swarmer has
368 covered half of the agar plate.

369 **Dextran Sulfate Sodium (DSS) induced acute colitis in conventional and gnotobiotic mice.**

370 Four to six week old female C57BL/6 mice (Jackson Laboratories, Bar Harbor, ME; # 000664)
371 were purchased and co-housed for acclimatization at The Albert Einstein College of Medicine
372 vivarium for 2 weeks prior to randomization by coin toss as previously described²⁸. To induce
373 acute colitis, mice were administered 3% (w/v) DSS (MW 36-50 KDa) (MP Biomedicals, LLC;
374 Cat. no. 160110) in animal facility drinking water throughout the course of the experiment. By
375 contrast, the control group or the normal mice always received animal facility drinking water. To
376 determine the effect of swarming and swarming deficient strains during colitis, mice were orally
377 gavaged with 100 μ L ($\sim 4 \times 10^9$ CFU/mL) test bacteria or LB as vehicle, daily for 9-12 days until
378 the weight of vehicle group dropped $>20\%$. Daily gavage of bacterial strains absolutely required
379 use of unwashed bacterial strains grown in fresh LB ($OD_{600} \sim 1.0$). In dose-optimization studies,
380 bacterial dilutions were prepared in its own spent medium to vary cell number as the only
381 determinant factor. Mice underwent daily monitoring for body weight, clinical signs and
382 symptoms (e.g., occult blood, diarrhea, activity), gross water consumption (measuring water
383 marked level), and visual inspection of rectal mucosa. At the end of the experiment, mice were
384 euthanized using isoflurane anesthesia and intestines harvested for histopathology. The histology
385 slides were prepared using a swiss role technique of intestines embedded in paraffin as previously
386 published²⁹. Scoring of inflammatory pathology was based on a published reference with minor
387 modifications³⁰. The experimenter was not blinded to treatment allocation; however, the
388 pathologist (K. S.) evaluating histologic scores was blinded to treatment allocation. All studies

389 were approved by the Institute of Animal Studies at the Albert Einstein College of Medicine, INC
390 (IACUC # 20160706 and preceding protocols).

391 Colitis was induced in five-week old germ-free (GF) wildtype (WT) C57BL/6 mice under specific
392 pathogen free (SPF) conditions³¹ using 3% DSS in drinking water and treated with 100 μ L (~
393 4×10^9 CFU/mL) of test strain or LB as vehicle for 7 days when most mice had >10% weight drop.
394 Mice were euthanized by CO₂ asphyxiation and histology specimens were prepared using swiss
395 roll technique. Scoring of inflammatory pathology was based on a published reference with minor
396 modifications³⁰. All GF mouse protocols were approved by the Institutional Animal Care and Use
397 Committee of the University of Florida (IACUC#201308038). The experimenter (ZH, CJ) was not
398 blinded to treatment allocation; however, the pathologist (KS) evaluating histologic scores was
399 blinded to treatment allocation. In addition, a second pathologist (QL), randomly re-read a subset
400 of the colitis histology slides which had a high correlation with original pathologist read (KS)
401 (Spearman $\rho = 0.96$, 95% CI 0.92 – 0.98, $P < 0.0001$, two-tailed).

402 **DSS-induced intestinal injury recovery model.** In a study to determine the healing effect of SM3
403 in colitis, C57BL/6 mice were administered 3% DSS in drinking water for 7 days (when most mice
404 had a weight loss >10% of their pre-DSS exposure weight). Subsequently, mice received animal
405 facility drinking water without DSS and were further randomized by coin-toss to a treatment group
406 delivered 4×10^9 CFU/mL of bacterial cells or LB by oral gavage for 5 days. Colon samples were
407 prepared for Hematoxylin-Eosin (H&E) staining and histology and processed as described above.
408 The precise number of mice used for each experiment are stated in the Figure legends and are
409 visible as separate plots in the graph. In the preliminary experiments (see Fig. 2d and 4c), the
410 computed means (\pm SD's) of the inflammation score for vehicle [7.28 – 9.28 (+ 1.77 – 2.4)] and
411 wildtype bacteria gavaged mice [2.59–5.66 (+ 1.31 – 3.2)] allowed for determination of the D

412 value (~ ranging between 2-3). The exact sample size was determined under consideration of the
413 D value, available mice per order, and ethical aspects (implementing replication studies, use of
414 coin toss 1:1 randomization, and cage space at any given time point) as well as an assumed
415 estimated inflation factor of $\leq 10\%$. For certain experiments, if insufficient number of mice were
416 available for a reliable significance prediction, biologically independent repetition experiments
417 were performed and data pooled for analysis (e.g., Fig. 2a-f, Fig. 4a-e).

418 **Construction of transposon mutants.** In order to generate an isogenic swarming deficient strain
419 of SM3, we adopted an *in vivo* transposition approach using pSAM_Ec with some modifications³².
420 pSAM_Ec was a gift from Matthew Mulvey (Addgene plasmid #102939;
421 <http://n2t.net/addgene:102939>; RRID:Addgene_102939). In short, donor strain –
422 EcS17/pSAM_Ec was grown from an overnight culture in pre-mating medium (M9 salts
423 containing 40 μ g/mL threonine and proline, 1 μ g/mL of thiamine) with 0.2% glucose until mid-
424 exponential phase (OD₆₀₀ 0.5-0.6). Similarly, the recipient strain SM3 was grown in pre-mating
425 medium containing 0.4% lactose until early exponential phase (OD₆₀₀ 0.2-0.3). After heat shock
426 treatment of the recipient strain at 50°C for 30 minutes the cell density of SM3 was scaled up to
427 obtain similar number of cells as that of the donor strain. For conjugation, 750 μ L of both the
428 strains were mixed, the cells were washed twice in M9 salts and re-suspended again in the same
429 medium. The mixture of donor and recipient was placed on a sterile 0.45 μ m membrane disc
430 (Millipore) rested on mating agar plate (1x M9-thr-pro-thi-glucose agar) and incubated upright at
431 37°C overnight. Next day, the cells were dislodged from the membrane in M9 medium by
432 vortexing and plated on selective agar medium (1x M9-threonine-glucose-kanamycin agar)
433 containing kanamycin. Individual colonies were spotted on LB swarm agar plate to screen non-
434 swarming or swarming deficient isogenic strain of SM3. The presence of transposon was

435 confirmed by using transposon specific primer while the location of transposon insertion was
436 verified by APPCR³³ followed by Sanger sequencing and mapping into the SM3 genome
437 (Extended Data Table 1 & 2).

438 **16S rRNA profiling to identify shift in colon microbiome.** 16S rRNA meta-analyses of the fecal
439 samples from mice were conducted at Wright Labs, LLC. Fecal samples were shipped to Wright
440 Labs, LLC on dry ice, and underwent DNA isolation using a Qiagen DNeasy Powersoil DNA
441 Isolation kit following the manufacturer's instructions (Qiagen, Frederick, MD). DNA was
442 quantified and checked for its quality using the double stranded DNA high sensitivity assay on the
443 Qubit 2.0 Fluorometer (Life Technologies, Carlsbad, CA). The 16S rRNA gene was amplified
444 using Illumina iTag Polymerase Chain Reactions (PCR) based on the Earth Microbiome Project's
445 16S rRNA amplification protocol³⁴. Amplified DNA was pooled, gel purified at ~400bp and
446 multiplexed with other pure libraries to form a sequencing library normalized to the final
447 concentration of library observed within each sample. The sequencing library was sequenced using
448 an Illumina MiSeq V2 500 cycle kit cassette with 16S rRNA library sequencing primers set for
449 250 basepair (bp) paired-end reads at Laragen Inc (Culver City, CA). The paired-end sequences
450 were merged with a minimum overlap of 200 bases, trimmed at a length of 251 bp, and quality
451 filtered at an expected error of less than 0.5% using USEARCH³⁵. The reads were analyzed using
452 the QIIME 1.9.1 software package^{36,37}. Chimeric sequences were identified and assigned
453 operational taxonomic units (OTU) using UPARSE at 97% identity³⁸. The taxonomy was assigned
454 using the Greengenes 16S rRNA gene database (13.5 release)³⁹. Linear discriminant analysis
455 (LDA) Effect Size (LEfSe) analysis was conducted to identify significantly enriched taxa within
456 categorical groups of interest⁴⁰. For all comparisons, a Kruskal-Wallis alpha (α) was set at 0.05 to
457 identify significantly enriched taxa, and a pairwise Wilcoxon rank sum test was utilized to test

458 biological consistency across all subgroups ($\alpha = 0.05$). Linear discriminant analysis (LDA) was
459 calculated to determine effect size, and the 5 most strongly enriched taxa within each cohort were
460 plotted. Co-occurrence network analysis was conducted on an unrarified OTU table containing
461 bacterial abundance data from DSS+ SM3 treated samples and created within the Cytoscape plugin
462 Conet^{41,42}. A spearman's rho threshold of $|0.7|$ was implemented prior to network plotting.

463 **Measurement of microlevels of oxygen in mouse lumen.** Oxygen concentration in the mouse
464 lumen was assessed using a profiling oxygen microsensor (PresensIMP-PSt7-02) with a flat tip
465 that has the ability to detect in the range of 0-1400 μM oxygen with an accuracy of $\pm 3\%$. The
466 control or DSS treated mice were first anesthetized in isoflurane for at least 3 minutes, and then
467 the microsensor probe was inserted from the anal verge. The oxygen concentration was monitored
468 for one minute at different locations across the colon (0.5, 1 and 2 cm from the anus) using “Presens
469 Measurement Studio 2 (version 3.0.1.1413)”. In order to avoid damage of the probe and mucosa
470 while inserting through the anus, we used an Ethylenetetrafluoroethylene (ETFE) tube (outer
471 diameter: 1mm; inner diameter: 0.7 mm) to house the probe. The housing was retracted to expose
472 the probe in the designated location and cleaned before moving to the next location within the
473 colon.

474 **Consumption of residual oxygen on swarming plates.** Swarming plates were prepared as
475 described previously and a fine hole (3 mm \times 1mm) was made on the lid of the plate to fix a syringe
476 based oxygen microsensor probe (Presens, NTH-PSt7-02). After inoculation of the test bacterial
477 culture, the probe was inserted into the swarming agar medium through the hole on the lid, finely
478 adjusted using a manual micromanipulator (Presens) and then sealed using silicon oil. The side of
479 the Petri dish was sealed using parafilm, and this whole unit was placed in the indigenously built
480 environmental controlled incubator at 37°C. The oxygen consumption within the agar plate over

481 time was monitored every 5 minutes for 20 hours using “Presens Measurement Studio 2”. The
482 average oxygen consumption rate in a sealed container was calculated by dividing the change in
483 oxygen concentration with time at which the oxygen levels reached a plateau phase. Consistently,
484 we have observed that during swarming activity of SM3, the plateau phase stabilizes at an oxygen
485 concentration of 0.003 ppm. This validated that the system used in this study was properly sealed
486 from the outside environment.

487 **Swarming on mucosal surface.** We used colon tissue from mice that had received 3% DSS water
488 or water for 10 days to develop a mucosal race experiment. Normal or DSS treated mice were
489 euthanized, and the large intestines were cut open and cleaned to remove residual feces. After
490 rinsing thoroughly twice in 35% (v/v) ethanol and PBS, the intestines were sectioned into small
491 segments of around 1.5-2.5 cm each. A hybrid plate with sterile swimming agar (3 g/L) and hard
492 agar (15 g/L) was prepared, where one half of the plate had 1.5% agar and the other half was filled
493 with 0.3% agar containing LB. To make such hybrid agar plate, 1.5% agar was poured first and
494 once solidified half of the gel was removed using a sterilized spatula to fill the rest of the Petridish
495 with swimming agar. The tissue pieces were placed on 1.5% agar in a way so as to have one end
496 of the tissue precisely overlapping with the border between 1.5% agar and the swimming agar.
497 Overnight bacterial cultures were serially diluted 10^{12} times to reach cell concentration of 10^6
498 CFU/mL, 2 μ L of which was inoculated on a 2 mm \times 2 mm sterilized filter membrane (MF-
499 Millipore, 0.45 μ m). Bacterial cells adsorbed on membrane was then used as a source of inoculum
500 on the mucosal surface. This avoided wetting of tissue surface that may facilitate free swimming
501 and free flowing of bacterial cells on tissue surface. The motility of a swarming deficient and its
502 wild type was always compared using a piece of tissue that belonged to the same region of the
503 colon in mice. The plates were dried in the laminar hood for 20-30 minutes before incubating at

504 37°C and 40% RH overnight. Drying of plates allowed removal of excess moisture from the
505 topmost layer of the tissue. Time-lapse photos were captured to evaluate the time at which bacterial
506 test strain reached the other end of the intestinal tissue indicated by the swimming of bacteria on
507 0.3% LB agar. Distance travelled by the bacterial strain was measured in ImageJ according to the
508 pixel/length ratio. The motility rates were calculated as Distance travelled / Time duration in which
509 the test strain reached the swim agar.

510 **Statistical analysis.** *P* values of data were obtained by parametric or non-parametric methods, as
511 indicated in the figure legends, with 95% confidence interval (CI). Normality (Gaussian
512 distribution) was not assumed and for each dataset this was either tested for or transformed (e.g.,
513 log normality) to discern whether the data fit a Gaussian distribution. Through visual inspection,
514 sample size assessment, and tests for normality, a determination was made to use a parametric or
515 non-parametric statistical test, as indicated. All statistical tests, except where otherwise indicated,
516 were performed with Graph Pad Prism v.8.2.0; * $P < 0.05$, ** $P < 0.01$, *** $P < 0.001$; ns, not
517 significant. All plots are shown as mean and 95% CI except where otherwise indicated.

518 **Methods References**

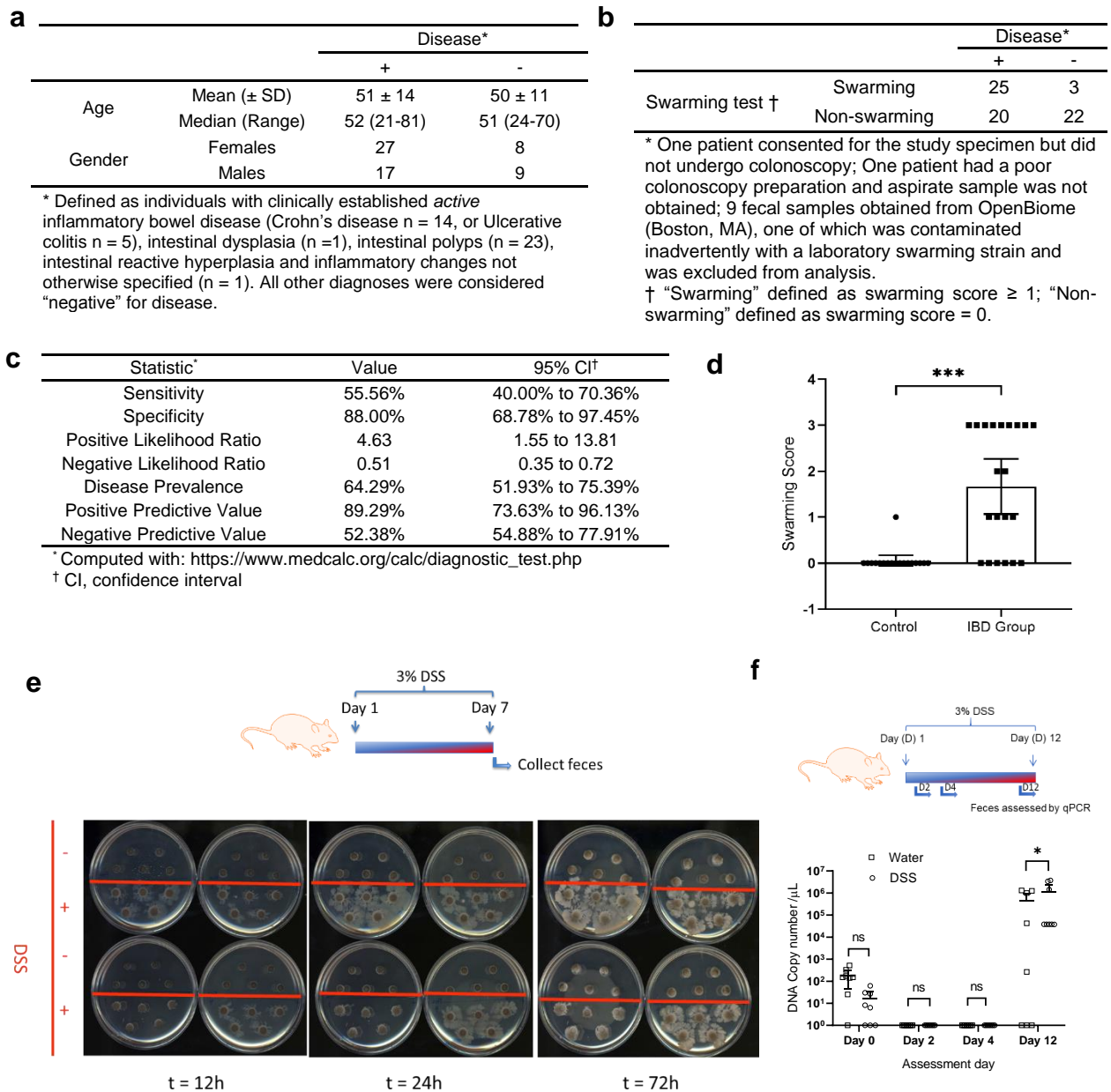
519

- 520 26 Munyaka, P. M., Sepehri, S., Ghia, J. E. & Khafipour, E. Carrageenan Gum and Adherent
521 Invasive Escherichia coli in a Piglet Model of Inflammatory Bowel Disease: Impact on
522 Intestinal Mucosa-associated Microbiota. *Frontiers in microbiology* **7**, 462,
523 doi:10.3389/fmicb.2016.00462 (2016).
- 524 27 Kearns, D. B. & Losick, R. Cell population heterogeneity during growth of Bacillus subtilis.
525 *Genes Dev* **19**, 3083-3094, doi:10.1101/gad.1373905 [doi] (2005).
- 526 28 Venkatesh, M. *et al.* Symbiotic bacterial metabolites regulate gastrointestinal barrier
527 function via the xenobiotic sensor PXR and Toll-like receptor 4. *Immunity* **41**, 296-310,
528 doi:10.1016/j.immuni.2014.06.014 (2014).
- 529 29 Whittam, C. G., Williams, A. D. & Williams, C. S. Murine Colitis modeling using Dextran
530 Sulfate Sodium (DSS). *J Vis Exp*, doi:10.3791/1652 (2010).
- 531 30 Erben, U. *et al.* A guide to histomorphological evaluation of intestinal inflammation in
532 mouse models. *Int J Clin Exp Pathol* **7**, 4557-4576 (2014).
- 533 31 McCafferty, J. *et al.* Stochastic changes over time and not founder effects drive cage
534 effects in microbial community assembly in a mouse model. *ISME J* **7**, 2116-2125,
535 doi:10.1038/ismej.2013.106 [doi] (2013).
- 536 32 Wiles, T. J. *et al.* Combining quantitative genetic footprinting and trait enrichment analysis
537 to identify fitness determinants of a bacterial pathogen. *PLoS Genet* **9**, e1003716,
538 doi:10.1371/journal.pgen.1003716 [doi] (2013).
- 539 33 Saavedra, J. T., Schwartzman, J. A. & Gilmore, M. S. Mapping Transposon Insertions in
540 Bacterial Genomes by Arbitrarily Primed PCR. *Curr Protoc Mol Biol* **118**, 15 15 11-15 15
541 15, doi:10.1002/cpmb.38 [doi] (2017).
- 542 34 Walters, W. *et al.* Improved Bacterial 16S rRNA Gene (V4 and V4-5) and Fungal Internal
543 Transcribed Spacer Marker Gene Primers for Microbial Community Surveys. *mSystems* **1**,
544 doi:10.1128/mSystems.00009-15 [doi] (2015).
- 545 35 Edgar, R. C. Search and clustering orders of magnitude faster than BLAST. *Bioinformatics*
546 **26**, 2460-2461, doi:10.1093/bioinformatics/btq461 [doi] (2010).
- 547 36 Caporaso, J. G. *et al.* QIIME allows analysis of high-throughput community sequencing
548 data. *Nat Methods* **7**, 335-336, doi:10.1038/nmeth.f.303 [doi] (2010).
- 549 37 Caporaso, J. G. *et al.* Global patterns of 16S rRNA diversity at a depth of millions of
550 sequences per sample. *Proc Natl Acad Sci U S A* **108 Suppl 1**, 4516-4522,
551 doi:10.1073/pnas.1000080107 [doi] (2011).
- 552 38 Edgar, R. C. UPARSE: highly accurate OTU sequences from microbial amplicon reads. *Nat*
553 *Methods* **10**, 996-998, doi:10.1038/nmeth.2604 [doi] (2013).
- 554 39 DeSantis, T. Z. *et al.* Greengenes, a chimera-checked 16S rRNA gene database and
555 workbench compatible with ARB. *Appl Environ Microbiol* **72**, 5069-5072,
556 doi:10.1128/AEM.03006-05 [doi] (2006).
- 557 40 Segata, N. *et al.* Metagenomic biomarker discovery and explanation. *Genome Biol* **12**, R60,
558 doi:10.1186/gb-2011-12-6-r60 (2011).
- 559 41 Shannon, P. *et al.* Cytoscape: a software environment for integrated models of
560 biomolecular interaction networks. *Genome Res* **13**, 2498-2504, doi:10.1101/gr.1239303
561 (2003).

- 562 42 Faust, K. & Raes, J. CoNet app: inference of biological association networks using
563 Cytoscape. *F1000Res* **5**, 1519, doi:10.12688/f1000research.9050.2 (2016).
- 564 43 Lee, K., Tosti, E. & Edlmann, W. Mouse models of DNA mismatch repair in cancer
565 research. *DNA Repair*, **38**, 140-146, doi:10.1016/j.dnarep.2015.11.015 (2016).
566

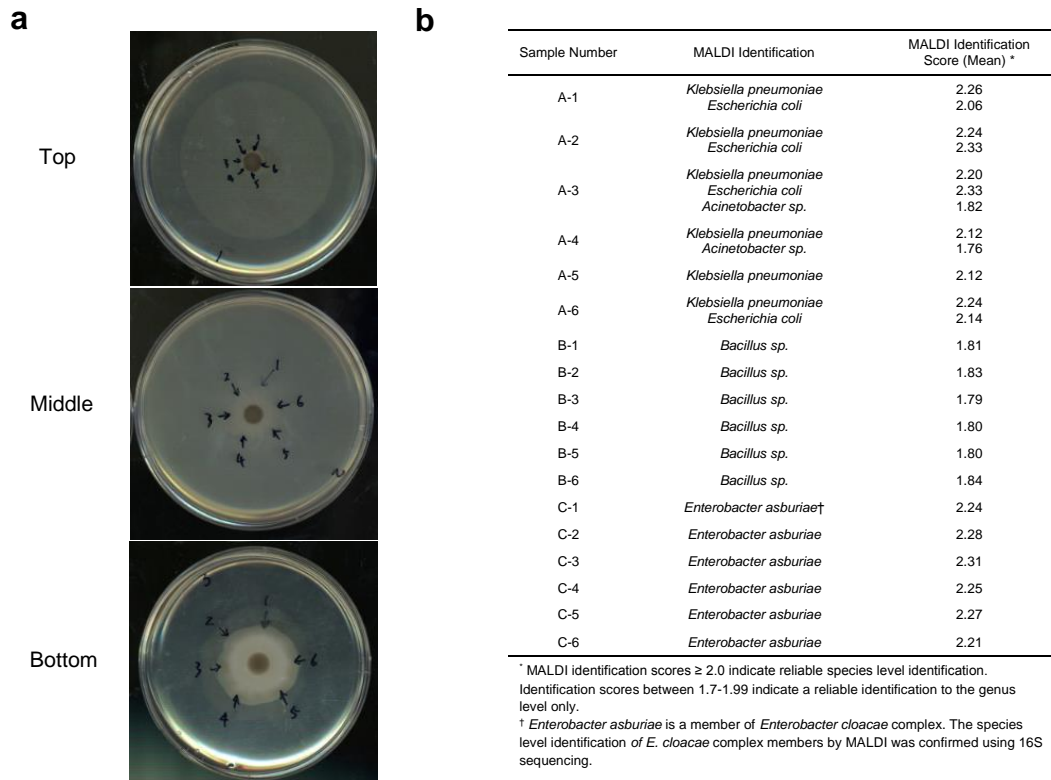
567 **Extended Data Figures**

Extended Data Figure 1



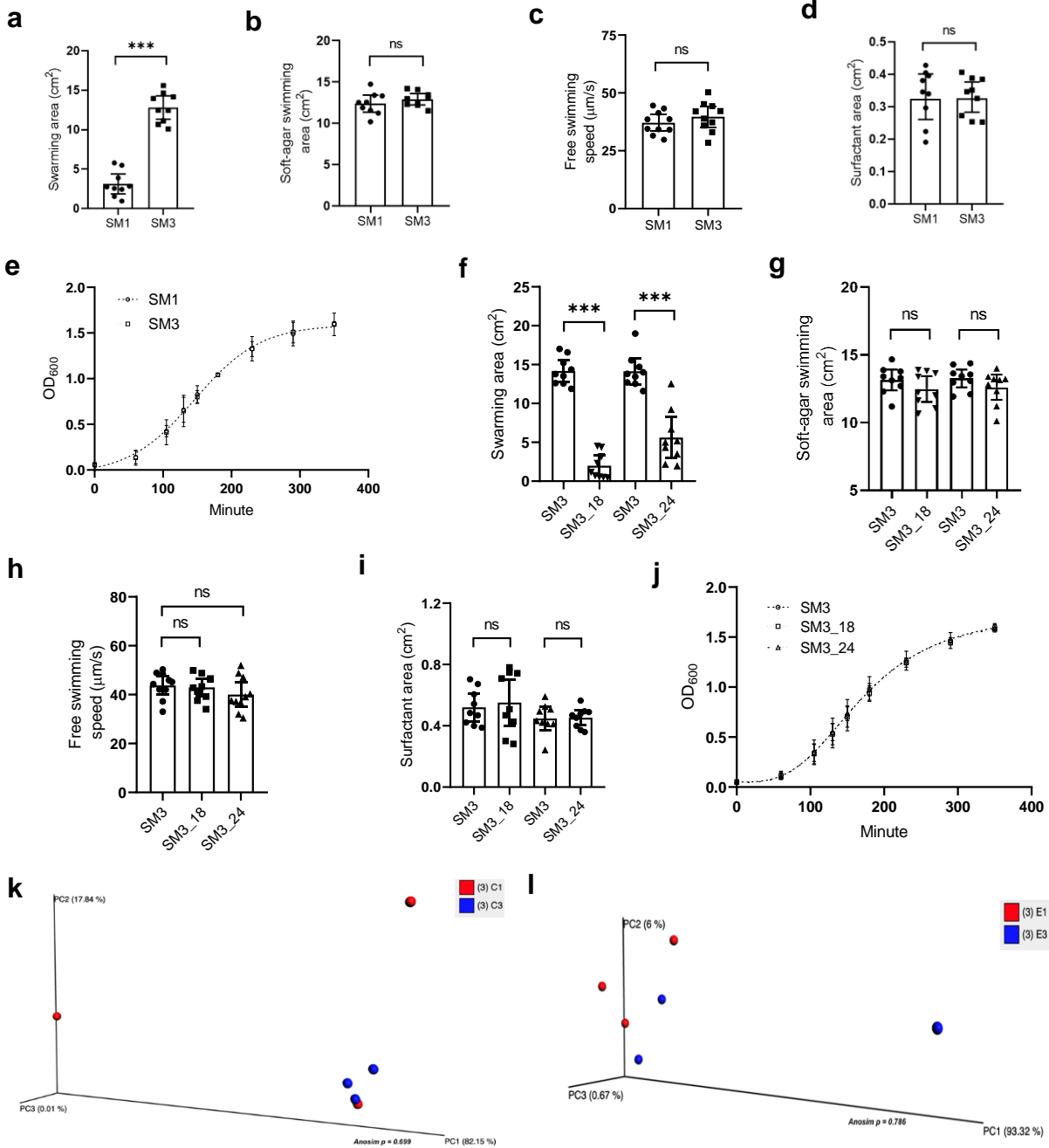
Extended Data Figure 1 | Effect of intestinal inflammation on bacterial swarming. **a-c**, Human colonoscopy aspirates (n = 45 intestinal disease; n = 25 non-disease) were spotted on 0.5% agar plates and the swarming assay performed. **a**, Colonoscopic washes were obtained from individuals with active intestinal disease and matched controls. Swarming assays performed using aspirates were binned by disease as defined both clinically and by intestinal histopathology, where available. **b**, Clinical demographics are described for the disease and non-disease population. **c**, Swarming assays' clinical test characteristics. **d**, Swarming assays (72h) of fecal samples collected from pigs with and without IBD. Swarming scores - 0: no swarming, 1: swarming within 72h, 2: swarming within 48h, 3: swarming within 24h or less (Control: n = 6; IBD: n = 7, each in triplicate, sampled from distinct regions of the semi-solid feces). **e**, C57BL/6 mice (8-week old) were exposed to water or DSS water for 7 days (n = 4 per group). Fecal samples of control group (above red line) and DSS group (below red line) were collected for swarming assay. Swarming plates were scanned at 12, 24 and 48 hours. **f**, In a separate experiment, C57BL/6 mice (8-week old) were exposed with water or DSS water for 12 days (n = 8 per group). Fecal samples were collected for DNA extraction and SM1/SM3-specific PCR analysis was performed, and DNA copy number ascertained. Unless otherwise noted, data represented as mean and 95% CI, significance tested using Fisher's Exact test.

Extended Data Figure 2



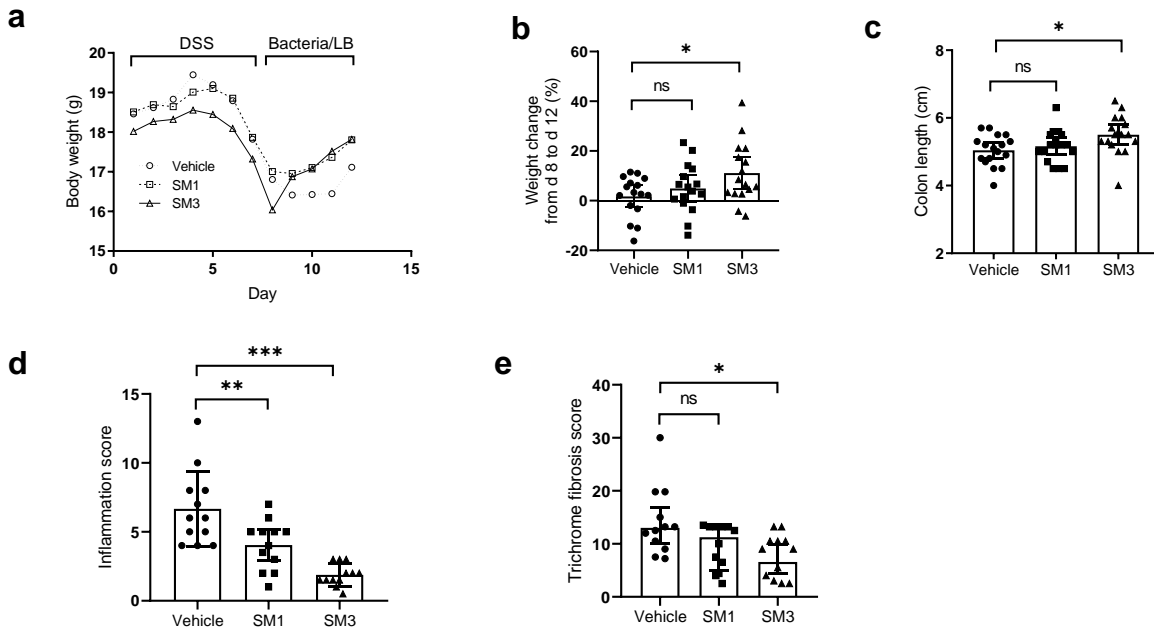
Extended Data Figure 2 | Identification of dominant swarming bacteria within a polymicrobial culture. a, 1:1 ratio mix of bacteria were used for swarming assay on 0.5% LB agar for 10 hours. *Top*: five non-swarming bacteria were mixed and applied on 0.5% agar. Six random picks as shown in arrows were placed on the edge of colony (1. *Klebsiella pneumoniae* 2. *Escherichia coli* 3. *Acinetobacter* sp. 4. *Bordetella hinzii* 5. *Staphylococcus xylosus*) and 1.5% LB agar streaks performed - single viable colonies were subjected to MALDI-TOF identification. *Middle*: five non-swarming bacteria as above plus two known swarming bacteria SM3 (*Enterobacter asburiae*) and *Bacillus* sp. were mixed, and experiment repeated as per *Top* panel. Six random picks as shown in arrows were placed on the edge of the complex. *Bottom*: five non-swarming bacteria as above plus one known swarming bacteria SM3 (*Enterobacter asburiae*). Six random picks as shown in arrows were placed on the edge of complex. **b**, Table showing results of MALDI-TOF identification of bacterial colonies isolated from swarming edge. A1-A6 are picks from **a Top**. B1-B6 from **a Middle**, and C1-C6 from **a Bottom**. “A” represents mix of bacterial species *Klebsiella pneumoniae*, *Escherichia coli*, *Acinetobacter* sp., and *Bordetella hinzii*, *Staphylococcus xylosus*; “B” represents mix of “A”, *Bacillus pumilus*, and SM3; “C” represents mix of “A” and SM3.

Extended Data Figure 3



Extended Data Figure 3 | Characterization of motility, growth, and surfactant production by *Enterobacter* sp. SM1, SM3 and its mutant strains. a-e, SM3 and SM1, swarming motility (a), soft-agar swimming motility (b), free swimming motility (c), surfactant production (d) and growth rate (e) (n = 3, each in triplicate except for e, n = 3, each in singlet). f-j, SM3 and mutants (SM3_18 and SM3_24), swarming motility (f), soft-agar swimming motility (g), free swimming motility (h), surfactant production (i), and growth rate (j) (n = 3, each in triplicate except for j, n = 3, each in singlet). k-l, Principal Coordinate Analysis (PCoA) plots of weighted Jaccard distance generated to determine global differences in expression of virulence and multi-drug resistance associated genes between cells collected from the center (k) and edge (l) of swarming colonies of SM1 and SM3 on agar. Unless otherwise noted, data are presented as mean and 95% CI, and significance tested using a two-tailed Student's t-test. h, significance tested using one-way ANOVA followed by Tukey's post hoc test. k-l, significance tested using ANOSIM showing no significant difference between the tested groups $p = 0.699$ (k) and 0.786 (l). C1, center of SM1; C3, center of SM3; E1, edge of SM1 and E3, edge of SM3.

Extended Data Figure 4

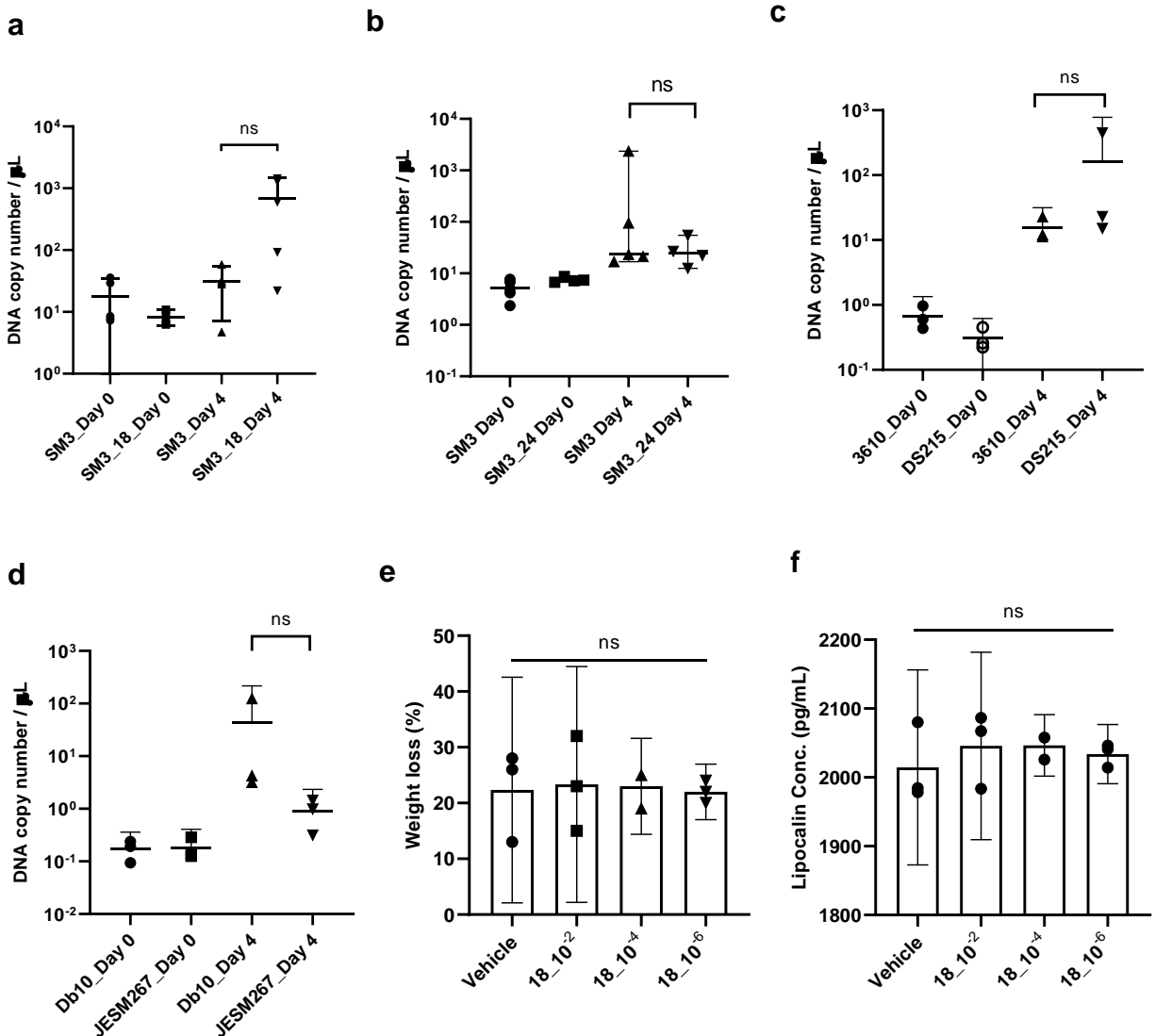


Extended Data Figure 4 | Effect of *Enterobacter* sp. SM1 or SM3 strain on DSS induced colitis in C57BL/6 mice during recovery phase. 8-week old mice were exposed to DSS water for 7 days. On day 8, DSS water was replaced with drinking water and mice were administered vehicle (LB), SM3 or SM1 for 5 days. **a-e**, indicates day by day weight change (**a**), day 8 to day 12 weight change (**b**), colon length (**c**), inflammation score (**d**), and trichrome fibrosis score (**e**) (n = 16 per treatment group except for **d** and **e**, four colon specimens per group were used for other experiments). Unless otherwise noted, data represented as mean and 95% CI, and significance tested using one-way ANOVA followed by Tukey's post hoc test. **e**, data represented as median and interquartile range, and significance tested using Kruskal-Wallis followed by Dunn's multiple comparisons test.

568 **Extended Data Figure 5**

569

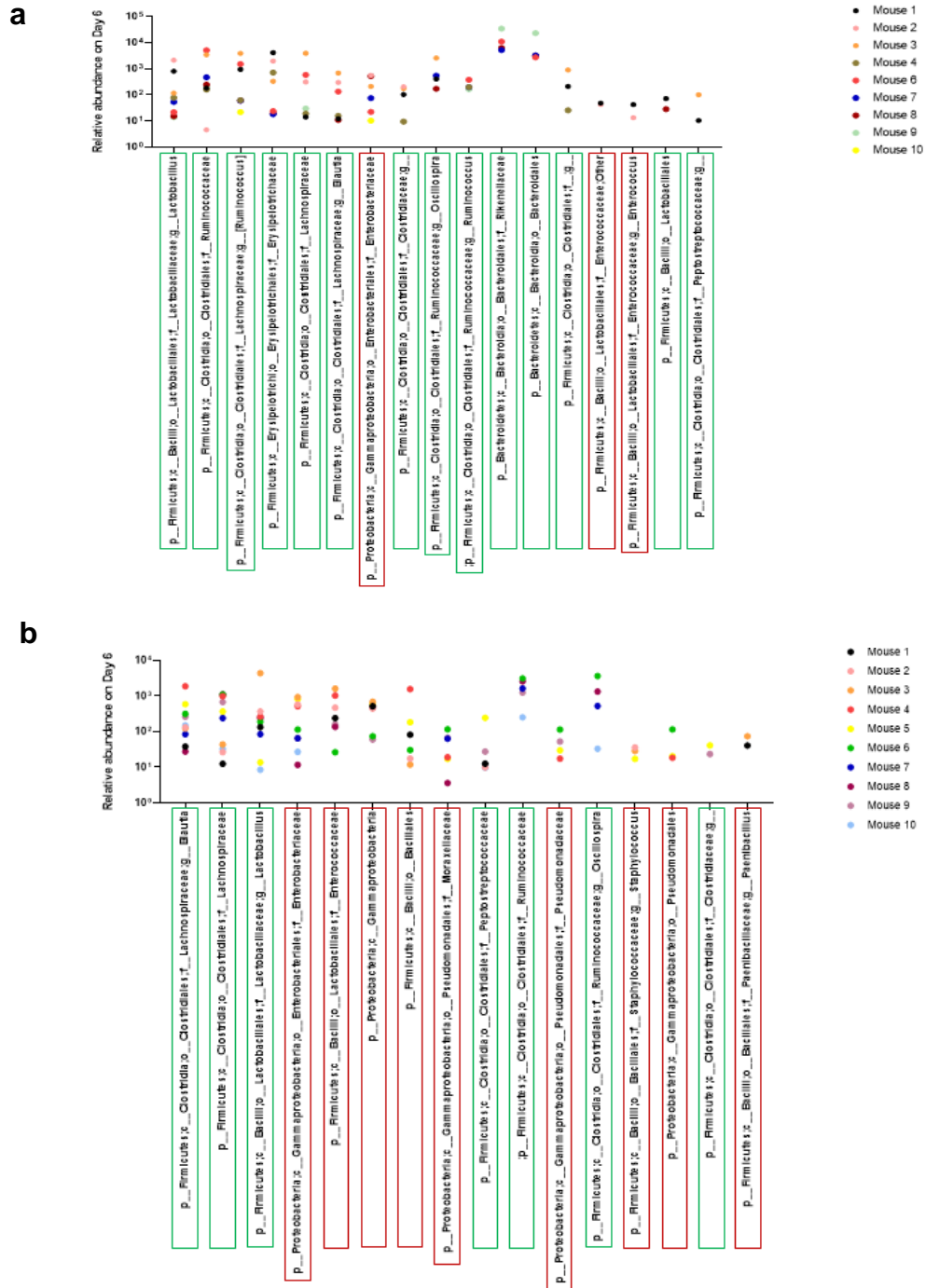
570



Extended Data Figure 5 | Bacterial enumeration in feces using qPCR and dose-optimization effect of SM3_18 on DSS induced colitis in C57BL/6 mice. a-d, 8-week old mice were exposed to DSS water for 4 days. Total DNA was extracted from feces collected on day 0 and day 4, processed and assessed using qPCR. 5ng of total DNA in conjunction with strain specific primers were used to quantify bacterial copy numbers. In each assay, DNA copy number/ μL was calculated based on an internal standard curve and compared between samples from mice treated with SM3 and SM3_18 (a), SM3 and SM3_24 (b), *B. subtilis* 3610 and DS215 (c) and *S. marcescens* Db10 and JESM267 (d) ($n \geq 3$ mice per treatment group, each performed as triplicate technical repeats). **e-f**, In a separate experiment, 8-week old mice were exposed to DSS water and treated with different dilutions (10^{-2} , 10^{-4} , 10^{-6}) of SM3_18 culture, which was grown in LB until 3 hours ($\text{O.D.}_{600} \approx 1.0$), for 10 days. **e**, Weight loss ($n = 3$ mice per treatment group) and **f**, Lipocalin concentration (pg/mL) ($n = 3$, each in triplicates). Data are represented as mean and 95% CI, and significance tested using Fisher's Exact test.

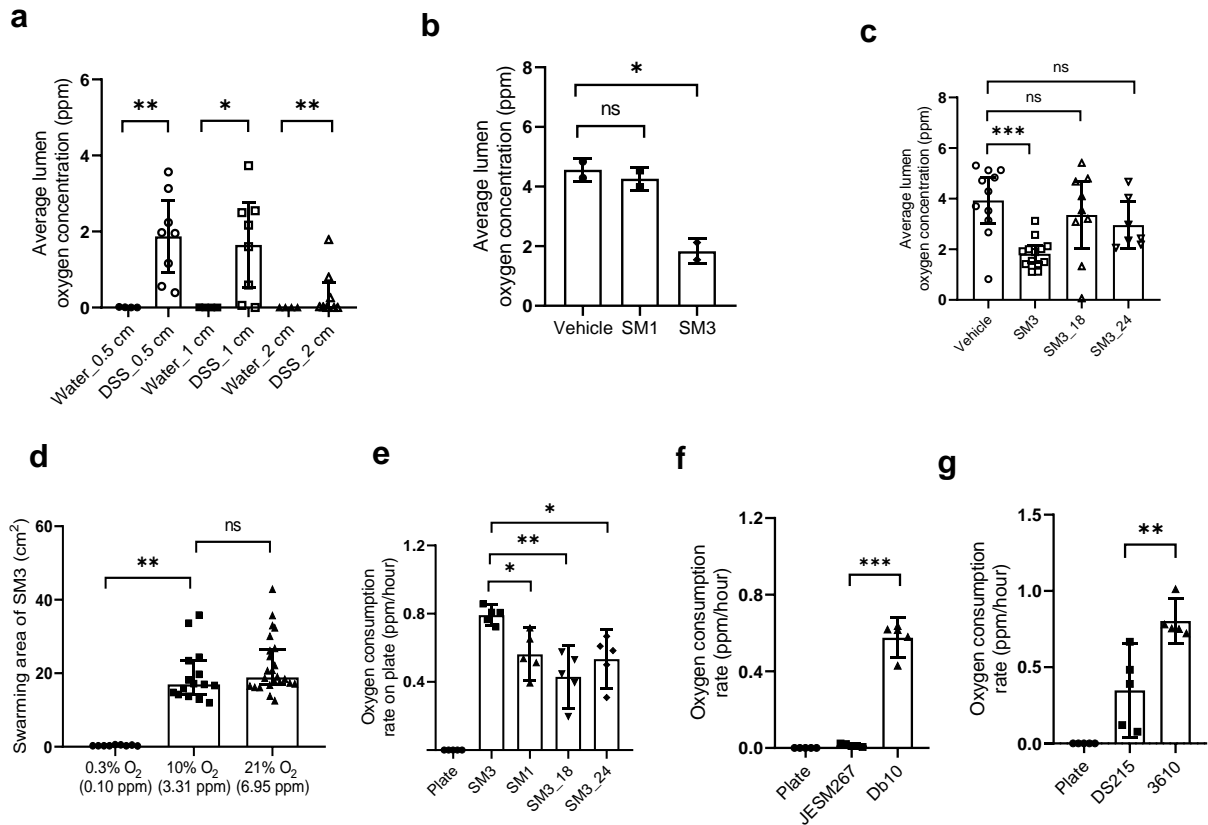
Extended Data Figure 6

571



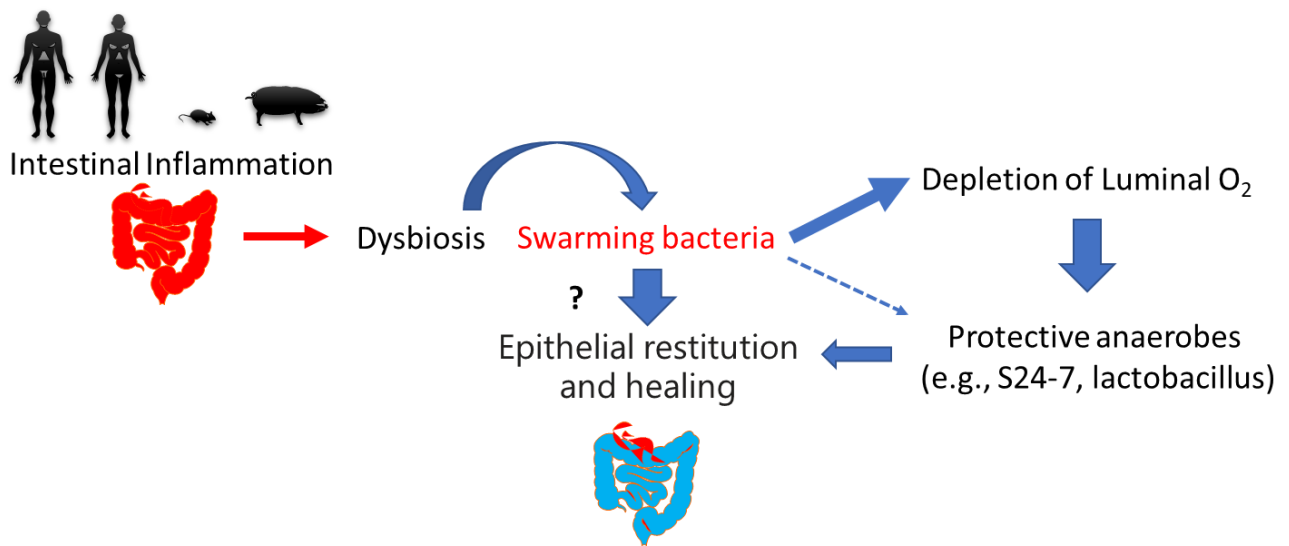
Extended Data Figure 6 | Relative abundance of different taxa in the feces of gnotobiotic mice. a-b, 16S rDNA profiling of feces samples from GF/SPF mice exposed to DSS and treated with SM3 (a) or vehicle (b) for 6 days were analyzed. The abundance of each taxa (represented as OTU) on Day 6 was normalized to its OTU values in feces collected on Day 0 or Day 3, in each individual mouse. All taxa with an abundance ratio > 10 and found at least in two individual mice are presented. Enrichment of these taxa indicates favorable conditions that allowed its growth during the course of the experiment, *in vivo*. Taxa highlighted in boxes are either microaerophilic and anaerobic (green) or aerobic or facultative anaerobic (red).

Extended Data Figure 7



Extended Data Figure 7 | Oxygen measurements *in vivo* and *in vitro* using a microsensor probe. **a**, C57BL/6 mice were exposed to water or DSS water for 10 days. Average lumen oxygen concentration (0.5, 1, and 2 cm from the anus) was measured (normal, $n = 4$; DSS, $n = 8$). **b**, C57BL/6 mice were exposed to DSS water and treated with SM3 and SM1 for 10 days. Average lumen oxygen concentration was measured in a single experiment ($n = 2$). **c**, In a separate experiment, C57BL/6 mice were exposed to DSS water and treated with SM3 or its mutants (SM3_18 or SM3_24) for 10 days. Average lumen oxygen concentration was measured ($n = 3$, at least 2 mice each separate experiment). **d**, The swarming area of SM3 on LB agar plate in 8 hours under different concentration of oxygen (0.3%: $n = 3$, each in triplicate; 10%: $n = 5$, each in triplicate; 21%: $n = 6$, each in quadruplicate). **e-g**, Oxygen consumption rate was measured for different strains: SM1, SM3, and its mutant strains (**e**); Db10 and JESM267 (**f**); 3610 and DS215 (**g**) on LB agar plate ($n = 5$, each in singlet). Plate indicates oxygen consumption rate in LB agar with no bacteria. Unless otherwise noted, data are presented as mean and 95% CI, and significance tested using one-way ANOVA followed by Tukey's post hoc test. **a**, data are presented as median and interquartile range, and significance tested using Kruskal-Wallis test. **b**, for 0.5 cm and 1 cm groups, significance tested using a two-tailed Student's *t*-test; for 2 cm groups, data are presented as median and interquartile range, and significance tested using Mann Whitney test.

Extended Data Figure 8



Extended Data Figure 8 | Schematic of proposed mechanism of cause and consequence of bacterial swarming during intestinal stress.

Acute intestinal stress (e.g., colitis), as opposed to a homeostatic colonic lumen, induces growth of bacteria with swarming properties. If the abundance of swarming bacteria has reached sufficient levels passing some threshold CFU, it may exhibit epithelial restitution and healing by a direct or indirect mechanism and reduce local luminal oxygen levels in the intestine creating a favorable environment for enrichment of anaerobes. The bloom of protective anaerobes such as belonging to family Bacteroidales S24-7 and Lactobacillaceae in turn correlates with the accelerated resolution of inflammation and healing in colitic mice. Thus, bacterial swarming is a protective response to intestinal stress and one that is garnered during the evolution of colitis. Dashed line represents a possible unknown link, “?” represent an underlying possible direct mechanism; CFU, Colony Forming Units.

572 Extended Data Tables

Extended Data Table 1 | Bacterial Strains isolated and used in this study

Bacterial strains identified from luminal contents and isolated on swarming agar*		
Strain Isolated	Swarming	Source
<i>Escherichia coli</i> #	+	Human IBD
<i>Escherichia coli</i> #	+	Human IBD
<i>Escherichia coli</i>	+	Human anal fistula
<i>Klebsiella pneumoniae</i>	+ †	Human IBD
<i>Klebsiella pneumoniae</i>	- ‡	Healthy Human
<i>Citrobacter koseri</i>	+	Human IBD
<i>Morganella morganii</i>	- §	Human IBD
<i>Serratia marcescens</i>	+	Human adenomatous polyp
<i>Proteus mirabilis</i>	+	Mouse colitis
<i>Proteus mirabilis</i>	+ ¶	Mouse colitis
<i>Enterobacter sp.</i> #	+	Mouse (DSS colitis)
<i>Enterobacter sp.</i> #	+	Mouse (TNBS colitis)

Bacterial strains used in this study		
Organism	Description	Reference
<i>Enterobacter sp.</i> SM1	A clinical isolate from feces of normal mice.	This study
Δ <i>motA</i> SM1	A flagella motor function abrogated mutant of SM1, <i>motA::kan</i>	This study
<i>Enterobacter sp.</i> SM3	A clinical isolate from feces of DSS-colitis mice.	This study
SM3_18	A transposon mutant of SM3, putative aerobactin synthesis gene <i>iucB::Tn::kan</i>	This study
SM3_24	A transposon mutant of SM3, putative isocitrate/isopropylmalate dehydrogenase/ADP-ribose pyrophosphate gene::Tn::kan	This study
<i>Serratia marcescens</i>	A clinical isolate from human adenomatous polyp.	This study
<i>Bacillus subtilis</i>		
3610	A wild-type isolate.	Kearns & Losick ²²
DS215	A swarming defective mutant of 3610, <i>swrA::tet</i>	Kearns et.al ²³
<i>Serratia marcescens</i>		
Db10	A wild-type isolate.	Pradel et.al ²⁴
JESM267	A serrawettin W2 defective mutant of Db10, <i>swrA::miniTn5-Sm</i>	Pradel et.al ²⁴
<i>Salmonella enterica</i> serovar Typhimurium		
ATCC 35659	A wild-type isolate.	
Δ <i>fliL</i>	A swarming deficient mutant of <i>S. enterica</i> , <i>fliL::FRT</i> .	This study

* Human or mouse feces was subject to the swarming assay and any swarm colony detected within 24 h was swabbed for strain identification. In addition, delayed swarmers were classified as negative but their swarm edge also yielded single species
† Feces from patient with clinically controlled Crohn's disease with moderate surfactant edge detected at 74 h
‡ Classified as non-swarmers, however, a very minimal surfactant edge present at 24h and no progression thereafter
§ Feces from patient with clinically controlled Crohn's disease with surfactant edge detected at 48h
||, ¶ Mouse model: *Msh2/-loxPTgfr2 loxp Villin-cre*⁴³
Also confirmed using Illumina Sequencing (PacBio)

Extended Data Table 2 | Primers used in this study

Primers	Sequence (5' → 3')	Description
MotA_Up_F	AGCAGAATATTCACGCTTCCA	Forward primer used to amplify <i>motA</i> upstream flanking region from SM1 genomic DNA
MotA_Up_R (BamHI)	TAAT <u>GGATCC</u> GTAACCTAATAAGATAAGCACGACATCA *	Reverse primer used to amplify <i>motA</i> upstream flanking region from SM1 genomic DNA
MotA_Dn_F(EcoRI)	TAAT <u>GAATTC</u> CGATCGGGTTGAGTTTG	Forward primer used to amplify <i>motA</i> downstream flanking region from SM1 genomic DNA
MotA_Dn_R	CGTTCTGGCTGTCGATAAT	Reverse primer used to amplify <i>motA</i> downstream flanking region from SM1 genomic DNA
Kan_F(BamHI)	TAAT <u>GGATCC</u> ATGGCTAAAATGAGAATATCACC	Forward primer used to amplify Kanamycin cassette from pCAM48
Kan_R(EcoRI)	TAAT <u>GAATTC</u> CTAAAACAATTCATCCAGTAAAATAT	Reverse primer used to amplify Kanamycin cassette from pCAM48
MotA_Up_seq_ver	AGCGAGAAAAGCATTGTTC	Sequencing primer to verify <i>motA</i> deletion at the 5' end in SM1
MotA_Dn_seq_ver	ATCATCAAGCCCACCTACCA	Sequencing primer to verify <i>motA</i> deletion at the 3' end in SM1
Just_F1	GAAGAACCGCAGTATCCCGA	Forward primer for SM1 and SM3 strain specific PCR verification
Just_R1	AGTGTGCTGCGAACGTAAGG	Reverse primer for SM1 and SM3 strain specific PCR verification
pSAM_Tn_det_F	CTGAATGAACTGCAGGACGA	Forward primer to verify transposon insertion in SM3 transposon mutants
pSAM_Tn_det_R	CTGGCAGTTCCTACTCTCG	Reverse primer to verify transposon insertion in SM3 transposon mutants
pSAM_Tn_ver_R	GCTTGCTGTCCATAAAACC	Transposon specific primer to identify its location in SM3 mutant during APPCR (cycle 1) †
pSAM_Tn_ver_F	GCTCTCTGAGTAGGACAAA	Transposon specific primer to identify its location in SM3 mutant during APPCR (cycle 1)
Ran3_APPCR	GTTCTACACGAGTCACTGCAGGGTGACGCAG ‡	Random primer to identify transposon location in SM3 mutant during APPCR (cycle 1)
Ran5_APPCR	GTTCTACACGAGTCACTGCAGGTCTACACGG ‡	Random primer to identify transposon location in SM3 mutant during APPCR (cycle 1)
Fix_APPCR	GTTCTACACGAGTCACTGC	Primer specific to amplicon generated in APPCR (cycle 1)
pSAM_verF_APPCR2_b	CATAAACTGCCAGGCATCAA	Primer specific to amplicon generated in APPCR (cycle 1) and annealing within the transposon
SM3_18_for	GTGATGGCAATCGGAATATCG	Forward primer to confirm transposon insertion location in the mutant SM3_18
SM3_18_rev	GTTACAGTTCACCTCGTGAAG	Reverse primer to confirm transposon insertion location in the mutant SM3_18
SM3_24_for1	ATCGATACCTATGAAAAATGTTCTG	Forward primer to confirm transposon insertion location in the mutant SM3_24
SM3_24_rev1	ATTGTGCAATTATCCATGTTGTG	Reverse primer to confirm transposon insertion location in the mutant SM3_24
Sa.en_FliL_F_FRTKan	CACGGGATAATCAGCCAATAAGCAGTACCGAAACAGGAA GCCGTATCAGATGGTGTAGGCTGGAGCTGCTTC	Forward primer for <i>fliL</i> deletion in <i>Salmonella enterica</i>
Sa.en_FliL_R_FRTKan	CAGCCTGAGAAAGAATACTATCGCCATATCGTTACCGC AGAATAAAAGCATGGGAATTAGCCATGGTCC	Reverse primer for <i>fliL</i> deletion in <i>Salmonella enterica</i>
Sa.en_FliL_det_F	ACGCCAGAGGTAGCATGATT	Sequencing primer to verify <i>fliL</i> deletion at the 5' end in <i>Salmonella enterica</i>
Sa.en_FliL_det_R	CTTGCATACCGGGAGTG	Sequencing primer to verify <i>fliL</i> deletion at the 3' end in <i>Salmonella enterica</i>

* Underlined sequences represent restriction digestion site.

† APPCR, Arbitrary-Primed Polymerase Chain Reaction.

‡ Sequences in bold in the primers Ran3_APPCR and Ran5_APPCR represent sequence similarity to the primer Fix_APPCR.